"$0\nu\beta\beta$ Decay : Current Progress and future Prospects"

A Dissertation Thesis submitted in partial fulfillment of the requirements for the degree of

Masters Of Science (Physics)

to

Department Of Physical Sciences, TilkaManjhi Bhagalpur University, Bhagalpur, Bihar

By:

Name : Avijeet Palit

Uni. Roll: 225701021

Session: 2021-23

Reg. No: 182630415/18

Supervisor:

Prof. Pankaj Kumar

Department of Physics

T.N.B College,

Bhagalpur

2021-2023

Prof. Pankaj Kumar,
T.N.B College, Bhagalpur

Dept. Of Physics
T.N.B College, Bhagalpur

Certificate

This is to certify that Mr. Avijeet Palit worked under the supervision and guidance of Prof. Pankaj Kumar for his dissertation at the Department of Physics, T.N.B College, Bhagalpur. The dissertation, titled "Neutrinoless Double Beta Decay: Current Progress and Future Prospects," has been submitted to T.M.B.U. Bhagalpur for the partial fulfillment of the award of the degree of Masters Of Science in Physics. The dissertation is a record of his original work.

The undersigned certifies that no work presented in Mr. Avijeet Palit's dissertation has formed the basis of the award of any previous degree to him or, to the best of our knowledge, to anybody else. Furthermore, the dissertation has not been submitted by the candidate for any research degree/dissertation in any other university.

Mr. Avijeet Palit has demonstrated commendable dedication and proficiency in his research work. His exploration into the topic of Neutrinoless Double Beta Decay showcases a thorough understanding of the subject matter. The work contributes significantly to the current progress in the field and sheds light on future prospects.

It is also affirmed that Mr. Avijeet Palit, in habit and character, is a fit and proper person for the award of the degree of Masters Of Science in Physics. The dissertation is recommended for evaluation and consideration for the degree.

Prof. Pankaj Kumar
Department of Physics
T.N.B College, Bhagalpur - 812007

Acknowledgement

I am filled with gratitude as I express my sincere thanks to Prof. Pankaj Kumar, Department of Physics, T.N.B College, Bhagalpur, for his invaluable guidance and support throughout the journey of my dissertation on "Neutrinoless Double Beta Decay: Current Progress and Future Prospects."

Prof. Kumar's generosity in sparing his precious time and providing sincere help in shaping the direction of my dissertation on such a complex and fascinating topic is truly commendable. I extend my heartfelt appreciation for his continuous supervision, insightful discussions, and unwavering motivation. His mentorship played a pivotal role in the conduction, discussion, and preparation of the manuscript, ultimately enabling the successful completion of this work.

I would also like to express my gratitude to my seniors and friends for their valuable suggestions, which greatly contributed to solving intricate concepts related to Neutrinoless Double Beta Decay and refining the quality of my research.

In addition, I want to acknowledge the profound influence of my parents. Their care and unwavering support have been my pillars of strength, instilling in me the importance and power of knowledge. Without their guidance, this accomplishment on such a complex topic would not have been possible.

This dissertation stands as a testament to the collaborative efforts and support I have received from Prof. Pankaj Kumar, my peers, and my family, and I am sincerely thankful for their contributions to my academic journey.

Avijeet Palit
U.Roll: 225701021
Reg No: 182630415/2018
Masters Of Science(Physics)
Department of Physics
T.N.B College, Bhagalpur - 812007

ABSTRACT

This MSC thesis, covering developments up to August 2023, presents a thorough exploration of neutrinoless double-beta ($0\nu\beta\beta$) decay research. Examining both theoretical and experimental progress, the thesis addresses the intricate challenges associated with detecting this rare decay mode. It emphasizes ongoing efforts to enhance sensitivity, highlighting the importance of global collaboration and optimized strategies. Beyond technical details, the work delves into the profound implications for understanding fundamental aspects of neutrino physics, including mass, hierarchy, and broader particle physics phenomena. Recognizing the interdisciplinary nature of this pursuit, the thesis underscores the interconnectedness of various experiments, from tonne-scale detectors to collider searches and lattice QCD calculations. Positioned at the forefront of groundbreaking discoveries, this thesis contributes significantly to advancing our understanding of neutrinos and the universe, encapsulating the latest advancements in this dynamic field as of August 2023.

CONTENTS

1. INTRODUCTION

Discoveries related to neutrino oscillations, adiabatic lepton flavor transformation, and neutrino mass have provided initial indications of physics beyond the Standard Model (SM). While there is much left to learn about neutrinos, including their mass-generation mechanism, absolute mass scale, CP-transformation properties, and whether they are Majorana fermions, resolving these unknowns would enhance our understanding of underlying symmetries governing leptons, baryogenesis, and the Universe's evolution.

The observation of the SM-forbidden neutrinoless double-beta (0νββ) decay process would directly confirm lepton-number violation and the Majorana nature of neutrinos. Depending on the assumed mechanism, crucial information about underlying model parameters could be obtained. The potential models for 0νββ decay span from sub-eV neutrinos to multi-TeV heavy particles, with implications for particle physics and cosmology. Without assuming a specific decay mechanism, searches for 0νββ decay aim to demonstrate the breaking of a global conservation law of the SM by detecting lepton-number violation.

$$(A, Z) \rightarrow (A, Z+2) + 2\,e^- + 2\,\bar{\nu}_e + Q_{\beta\beta},$$

Double-beta (ββ) decay involves a transition from a parent nucleus (A, Z) to a daughter nucleus (A, Z + 2), with the two-neutrino double-beta (2νββ) decay mode releasing energy accompanied by two electrons and two electron-type antineutrinos. This SM-allowed decay has a typical half-life of >10^19 years.

$$(A, Z) \rightarrow (A, Z+2) + 2\,e^- + Q_{\beta\beta},$$

In contrast, the SM-forbidden 0νββ-decay mode, violating lepton number by two units (ΔL = 2), emits no neutrinos and is extremely challenging to detect. Previous attempts have yielded the best half-life limits of >10^26 years.

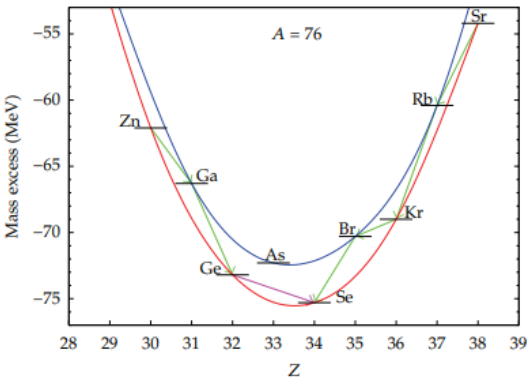

Fig 1: Illustrates the energy representation of the A=76 isobars, showcasing the distinctive features of the decay processes. The β-decay pathway, indicated by green arrows, is not feasible for the transition between 76Ge and 76Se due to energetic constraints. Consequently, the sole decay channel is the double beta decay (ββ), denoted by the pink arrow. The presence of two mass parabolas arises from the pairing interaction, influencing the energy levels of even Z—even N nuclei in comparison to odd Z—odd N nuclei. For odd A nuclei, a single mass parabola exists, and all single-beta transitions are energetically permissible.

The double-beta decay stands out as an exceptionally rare nuclear weak process, occurring specifically between two even-even isobars. The energetic hindrance preventing decay to the intermediate nucleus is a consequence of the pairing interaction, which causes a shift in the mass parabolas of both even-even and odd-odd

nuclei within a given isobaric chain. Consequently, the double-beta decay becomes observable primarily due to this pairing interaction, as illustrated in Figure 1.

The two-neutrino decay, initially proposed by Goeppert-Mayer in 1935, conserves lepton number and is characterized as a second-order weak process, accounting for its notably low rate. Its detection in a laboratory setting was only accomplished relatively recently in 1987. Subsequent measurements have been conducted on approximately a dozen nuclei, revealing lifetimes spanning the range of 10^18 to 10^22 years.

An alternative to this process is the neutrinoless double-beta decay (0νββ), introduced by Furry following the Majorana theory of the neutrino. Neutrinoless decay is contingent on the neutrino being a massive Majorana particle, necessitating an extension of the standard model of electroweak interactions. This extension is imperative because neutrinoless decay violates lepton number conservation. Therefore, the observation of double-beta decay without the emission of neutrinos would serve as an indication of the Majorana nature of the neutrino.

Currently, numerous experiments are either underway or anticipated in the near future to detect and firmly establish the nature of neutrinos. The most stringent limits on neutrino lifetime are around 10^25 years. Claims suggesting the existence of neutrinoless double-beta (0νββ) decay in the isotope 76Ge propose a half-life of approximately 2.2×10^25 years. This decay process is also crucial for exploring the absolute scale of neutrino masses, particularly if mediated by the mass mechanism, influencing the mass hierarchy The half-life, along with the effective Majorana neutrino mass determined by nuclear matrix elements (NME), is essential for predicting favorable decays and, upon detection, determining the neutrino mass scale and hierarchy.

Another noteworthy process is resonant double-electron capture, which could have lifetimes competitive with neutrinoless double-beta decay if there exists a degeneracy of atomic masses in the initial and final states at the eV level. However, current high-precision mass measurements have ruled out proposed candidates for this process. Similar to neutrinoless double-beta decay, the decay rate of resonant double-electron capture depends on the effective Majorana neutrino mass and the NME.

The experimental challenges of 0νββ-decay searches are matched by theoretical difficulties, particularly in understanding the nuclear physics aspects. Despite numerous review articles on 0νββ decay, our aim in this review is to highlight recent theoretical and experimental developments. Current experiments have reached a 0νββ-decay half-life (Tv1/2) limit in the range of 10^25–10^26 years, motivating a global effort to enhance sensitivity by two orders of magnitude in the ongoing search for this decay.

2.SCIENTIFIC MOTIVATION

Neutrinoless double beta decay (0νββ) investigations, using a nuclear approach, tackle various fundamental questions in subatomic physics and cosmology. These encompass:

• Is there a fundamental symmetry tied to Lepton Number?
• What is the source of the neutrino's mass? Are neutrinos Majorana fermions, i.e., their own antiparticles?
• Why does the universe have more matter than antimatter?
• What are the absolute masses of neutrinos, and how have they influenced the universe's evolution?

In 0νββ decay, two neutrons transform into two protons, emitting two electrons and no neutrinos, altering the lepton count by two units. In the Standard Model, lepton number L (specifically, the difference B − L of baryon and lepton number) is conserved. The observation of 0νββ decay would provide direct evidence of new physics, indicating that neutrino mass involves a Majorana component, suggesting neutrinos are self-conjugate particles. Additionally, this observation would imply new mechanisms for mass generation, distinct from those affecting other matter particles, possibly originating at very high energy scales. The detection of a "matter-creating" process like 0νββ decay would also support leptogenesis scenarios for generating the matter-antimatter asymmetry in the universe.

Ton-scale 0νββ decay searches aim to explore a broad range of lepton number violation mechanisms. These mechanisms span from high-scale seesaw scenarios linked to Grand Unified Theories to models influencing electroweak scale physics, near the TeV scale, and down to light (eV scale) right-handed neutrinos. The diverse physics involved enhances the discovery potential of 0νββ decay. However, the multitude of models makes it challenging to quantify the discovery potential of planned experiments using a universal metric.

This whitepaper employs various parameters to characterize the physics reach. Initially, focusing on a class of models where 0νββ is mediated by the exchange of three known light neutrinos, assuming they are Majorana particles, the decay rate is expressed as $G01|M0\nu|2|m\beta\beta|2$. Here, G01 is a phase space factor, M0ν is a nuclear matrix element, and $m\beta\beta = \sum i=1^3 Uei^2 mi$ represents the lepton number violating parameter. This parameter is determined partially by neutrino oscillation data. Ton-scale experiments aim to cover the entire inverted ordering region, corresponding to $m\beta\beta > (18.4 \pm 1.3)$ meV. Discovery is possible if the spectrum is inverted or if the lightest neutrino mass exceeds 50 meV, irrespective of the ordering. Falsifiable correlations arise with other neutrino mass probes, such as single beta decay and cosmology.

While it's common to present the physics reach of 0νββ searches in terms of mββ, it's crucial to note that this covers only one class of models for Majorana neutrino mass, where lepton number violation originates at a very high mass scale Λ. In many models with Majorana neutrinos, other sources of lepton number violation exist, leading to contributions to 0νββ not directly related to the exchange of light neutrinos. For instance, in left-right symmetric models, contributions from the exchange of heavy neutrinos, heavy W bosons, and charged scalars with masses in the few TeV range can occur. In general, at low energy, the effect of these heavy particles is captured by a set of $\Delta L = 2$ local operators of odd dimension (seven, nine, ...), suppressed by odd powers of the heavy mass scale Λ associated with lepton number violation ($1/\Lambda^3$, $1/\Lambda^5$, ...). This mirrors the Fermi theory of weak interactions, where the effect of W exchange is captured by the usual V − A current-current (dimension six) interaction, suppressed by $1/\Lambda^2$ew, with $\Lambda ew = 1/\sqrt{GF}$. The physics reach of current and future 0νββ searches is presented in Fig. 1 in terms of both mββ and the scale Λ associated with representative dimension-seven and dimension-nine operators [5], reaching well into the hundreds of TeV region, inaccessible to any other probe.

In summary, given the breadth of mechanisms and scales associated with lepton number violation, ton-scale searches for 0νββ have a significant discovery potential that extends beyond the "inverted mass ordering" region in mββ, covering a variety of models across the particle physics landscape. Other non-0νββ decay experimental efforts can complement results from 0νββ decay searches but do not diminish the need for further progress in 0νββ decay science.

Mass Ordering Determined – If the mass ordering is established, the inverted mass ordering could either be identified or become irrelevant. Even in the latter case, the normal order branch still extends to high mββ values. Furthermore, lepton-number-violating processes other than light neutrino exchange are not constrained by oscillations. At present, even with the normal mass ordering, the probability of discovering 0νββ decay is significant [6].

Cosmological Probes of $\Sigma \equiv \sum i=1^3 mi$ – Future efforts in observational cosmology aim to make the first measurement of Σ. An observation of $\Sigma < 100$ meV would effectively rule out the inverted mass ordering. However, cosmology does not distinguish the Majorana/Dirac character of the neutrino. A three-neutrino normal-ordering scenario with Σ near its minimum would not constrain other potential lepton-number-violating processes contributing to 0νββ decay. Cosmology, as a standard model of physics with many parameters to be deduced, must be tested in all possible ways. There are few complementary laboratory measurements that can directly test results from cosmology. Laboratory measurements of neutrino properties may provide such tests.

Neutrino Mass Found – If neutrino mass is observed in β decay, it will make the observation /non-observation of 0νββ decay even more exciting. A null 0νββ decay result might indicate Dirac neutrinos or, if lepton number violation is additionally observed in collider experiments, alternative / interfering mediation mechanisms or flavor symmetries driving mββ to be small.

Lepton Number Violation Observed at Collider Experiments – The LHC or other collider experiments might observe lepton number violation consistent with a heavy neutrino, LR symmetry, or other BSM physics. Such a result would be complementary to a discovery of 0νββ decay, leading to the interesting possibility of testing the underlying physics.

Sterile Neutrinos – If a convincing demonstration of a sterile neutrino is found, it will fit well into the Majorana neutrino paradigm. This will increase 0νββ decay interest. The new neutrino might contribute to 0νββ decay and significantly alter predicted mββ curves.The sensitivity regions accessible to experiments will remain.

Solar Mixing Angle – The interpretation of a limit or measurement of the rate of 0νββ decay in terms of neutrino mass would be aided by better measurement of θ12.

3.NEUTRINOLESS DOUBLE BETA DECAY AND NEW PHYSICS

The main feature of 0νββ decay is the violation of lepton number. In the modern standard model perspective, this is as important as the violation of the baryon number. In a very general context, we can imagine this process as a mechanism capable of creating electrons in a nuclear transition. It is evident that this transition is not necessarily due to the exchange of Majorana neutrinos as a leading contribution, although its observation would prove that neutrinos are self-conjugate particles.

Many extensions of the standard model generate Majorana neutrino masses and offer a plethora of 0νββ decay mechanisms, such as the exchange of right-handed W-bosons, SUSY superpartners with R-parity violating, leptoquarks, or Kaluza-Klein excitations, among others, which have been discussed in the literature. Possibilities to disentangle at least some of the possible mechanisms, e.g., those related to the existence of right-handed currents, rely on the analysis of angular correlations between the emitted electrons possible only in one of the future proposed searches, the study of the branching ratios of 0νββ decays to ground and excited states, a comparative study of the 0νββ decay and neutrinoless electron capture with the emission of a positron, and analysis of possible links with other lepton-flavor violating processes.

However, after the discovery of neutrino flavor oscillations, which prove that neutrinos are massive particles, the mass mechanism occupies a special place. It neatly relates the 0νββ decay to important parameters of neutrino physics, fixes clear experimental targets, and provides a clue to compare experiments on an equal footing, even when they present considerable differences from the methodological and technological points of view. The lifetime of the 0νββ decay is related to the so-called effective Majorana neutrino mass, defined by the following equation:

$$\langle m_\nu \rangle = \left| \sum_k U_{ek}^2 m_k \right| = \left| \sum_k |U_{ek}|^2 m_k e^{i\alpha_k} \right|.$$

The crucial parameter contains the three neutrino masses mk, the elements of the first row of the neutrino mixing matrix U_{ek}, and the unknown CP-violating Majorana phases α_k; only two of them have a physical meaning, allowing for the cancellation of terms: mν could be smaller than any of the mk. Thanks to the information from oscillations, it is useful to express mν in terms of three unknown quantities: the mass scale, represented by the mass of the lightest neutrino m_{min}, and the two Majorana phases. Three mass patterns are commonly distinguished: normal hierarchy, where m1 < m2 < m3, inverted hierarchy, where m3 < m1 < m2, and the quasi degenerate spectrum, where the differences between the masses are small with respect to their absolute values. The neutrino mass ordering is currently unknown, and the 0νββ decay has the potential to provide this essential information. If experimentally established that mν ≥ 50 meV, one can conclude that the quasi degenerate pattern is correct and extract an allowed range of m_{min} values. If mν lies in the range 20–50 meV, the pattern is likely an inverted hierarchy, although the normal hierarchy cannot be excluded if the lightest neutrino mass sits on the far right of the allowed band. If determined that mν < 20 meV is nonvanishing, the conclusion would be that the normal-hierarchy pattern holds. Therefore, 0νββ is crucial for understanding fundamental aspects of elementary particle physics and contributing to the solution of hot astroparticle and cosmological problems related to the neutrino mass scale and nature.

4. PARTICLE PHYSICS ASPECTS

4.1 Why Look for Lepton-Number Violation?

The searches for 0νββ decay aim to detect lepton-number violation, which is typically absent in the Standard Model (SM) unless additional symmetries enforce lepton number conservation. The introduction of theories beyond the SM often involves lepton-number violation through a $\Delta L = 2$ Majorana mass term for standard or new neutrinos. Grand Unified Theories (GUTs), for instance, introduce new neutral fermions, such as the 16-dimensional spinorial representation of SO(10) that includes all SM particles of a generation along with a right-handed neutrino.Models like left–right symmetric theories and those gauging the difference of baryon and lepton numbers (B − L) also include right-handed neutrinos with Majorana masses. The presence of right-handed neutrinos implies the existence of light massive Majorana neutrinos through the seesaw mechanism. R-parity-violating supersymmetry is an example without right-handed neutrinos, generating Majorana neutrino masses at the loop level through specific terms in the Lagrangian.

Lepton-number violation is strongly supported by theoretical considerations, but its strength depends on the model and requires experimental probing. Predictions within well-motivated frameworks specify scales to be tested, such as the minimal effective mass in the inverted mass ordering of light neutrinos. Observables like the sum of neutrino masses or cross sections for specific signals at the LHC provide avenues for experimental verification and differentiation of mechanisms.

The observation that there is matter in the Universe suggests the existence of mechanisms beyond the SM to create matter. 0νββ decay, as a process creating matter, becomes crucial in demonstrating ideas about baryogenesis.Considering the energy scales probed by lepton-number violation and proton decay, the 0νββ-decay half-life in the standard light-neutrino mechanism is proportional to Λ^2, where is the scale of neutrino mass generation. In contrast, proton decay half-lives are proportional to the GUT scale , with different powers for non supersymmetric and supersymmetric decay modes (Λ^4 and Λ^5, respectively). These scales present distinct challenges for experimental testing, and generalizing model-independent statements is difficult.

4.2 Neutrino Mass and Neutrinoless Double-Beta Decay

The observation of neutrino oscillations demonstrated that neutrinos have mass. The two main consequences from the impressive experimental progress in the last two decades are that (a) the two different mass-squared differences imply that all neutrino masses are different, with at least two of them being nonzero, and (b) lepton mixing is large. The scalar and fermion content of the SM does not allow for neutrino masses; hence, neutrino oscillations imply physics beyond the SM. It is highly non trivial to explain this so-called New Physics within a simple paradigm. In this three-Majorana-neutrino paradigm, all phenomena related to neutrino physics are generated by the neutrino mass matrix $m_\nu = U \mathrm{diag}(m_1, m_2, m_3) U^T$, where m_i are the real and positive neutrino masses and U is the Pontecorvo–Maki–Nakagawa–Sakata (PMNS) matrix containing three mixing angles and three CP phases (one Dirac and two Majorana phases). It is important to note that the smallest neutrino mass is not currently known and that two options for neutrino mass ordering exist: $m_3 > m_2 > m_1$ (normal ordering) and $m_2 > m_1 > m_3$ (inverted ordering). The cases in which the lightest neutrino mass is much smaller than the heavier masses are denoted the normal or inverted hierarchy. There are altogether nine physical parameters in m_ν , seven of which appear in the effective mass:

$$\langle m_{\beta\beta} \rangle = \left| U_{ei}^2 \, m_i \right| .$$

All seven, except for the two Majorana phases α and β, can be determined by other means—the absolute values of U from neutrino oscillations and the neutrino mass scale from direct kinematic searches or cosmology.We note that this formula holds in the three-Majorana-neutrino paradigm, in which all neutrino phenomenology is determined by three Majorana neutrinos. In the light-neutrino exchange model, which has hitherto been the most espoused in the physics community, the 0νββ-decay half-life is:

$$T_{1/2}^{0\nu} = \left(G\,|\mathcal{M}|^2\,\langle m_{\beta\beta}\rangle^2\right)^{-1} \simeq 10^{27-28}\left(\frac{0.01\ \text{eV}}{\langle m_{\beta\beta}\rangle}\right)^2 \text{years.}$$

In this interpretation of 0νββ decay, it is a neutrino mass experiment under the assumption that no other mechanism contributes to lepton-number violation and that the neutrinos are Majorana particles. In Equation above, the phase-space factor G $\propto$ Q^5 ββ is of the order of 10^−25 (year·eV^2)$^{-1}$. For the NME, M, the approximation |M|^ 2 ~ 10 is used. From the experimental discussion, below, it is clear that tonne-scale experiments are needed to probe the physically interesting regime of $T_{0\nu}$ 1/2 ~ 10^28 years and mββ ~ 0.01 eV. The current limits on mββ are approximately 0.2 eV. For the SM V –A weak interaction, it is worth noting that any observable connection to the Majorana nature of the neutrinos is suppressed by the square of the neutrino mass divided by the energy scale of the process (19). This is why T0ν 1/2 is so large compared with that in the 2νββ-decay process. The neutrino mass can also be probed by direct kinematic searches, such as the KATRIN and ECHo experiments, as well as by cosmological observations. The kinematic searches and cosmological observations are sensitive to:

$$m_\beta = \sqrt{|U_{ei}|^2\, m_i^2} \ \text{ and } \ \Sigma = m_1 + m_2 + m_3,$$

respectively. While the direct kinematic searches provide the most model-independent approach to test the neutrino mass, they give the weakest limits; the projected mβ sensitivity in the KATRIN experiment is 0.2 eV. Cosmology provides the strongest mass limits in the sum of the neutrino masses. But they depend on the data sets that need to be combined in order to break the degeneracies of the many cosmological parameters. The limits also become weaker when one departs from the seven parameter framework of CDM (Lambda cold dark matter model) plus neutrino mass (denoted CDM+mν) to frameworks with more cosmological parameters. The neutrino mass limits in exotic models of modified gravity are difficult to quantify, but are expected to be weaker as well. The current conservative limits are approximately 0.3 eV. The readers are referred to the latest Planck data release for a detailed analysis of the cosmic microwave background and other related data. It is noteworthy that a neutrino mass signal is quite likely in future observations within the CDM+mν framework, as well as in other moderate extensions, especially if the Planck data are combined with the future Euclid and Square Kilometer Array data. This exciting prospect distinguishes the cosmological observations from other approaches. 2 .Nevertheless, we repeat that the limits and constraints are hard to quantify in exotic modifications of the minimal CDM+mν model; the combination of different data sets is prone to misinterpretations when a multitude of systematic effects are present.

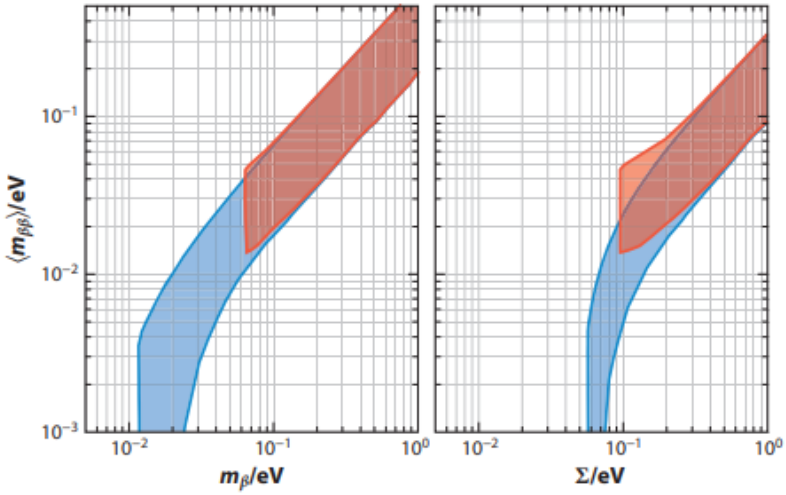

Fig 2: The effective mass mββ versus the kinematic neutrino mass observable mβ , and the cosmological observable.The neutrino oscillation parameters are varied within their 3σ ranges. The blue (red) area is for the normal (inverted) mass ordering.

The smallest neutrino mass and the Majorana phases are not known. Varying them allows us to plot the three mass observables against each other, which illustrates nicely the complementarity of the different neutrino mass probes in Figure 2. In the scenario of normal mass ordering with hierarchical masses, mββ is of the order of meV and can even vanish. In the inverted-ordering scenario, there is a minimum value of approximately 0.013 eV . This value represents a physics goal for the current and upcoming 0νββ-decay experiments. The current global fits of neutrino oscillation data favor the normal mass ordering over the inverted one by more than 3σ . Small tensions in the values of the oscillation parameters m2 31 and θ13 obtained from the long-baseline and reactor experiments contribute to this preference, as does an excess of upward-going electron-like events in the Super-Kamiokande atmospheric neutrino data. The current situation may change; nevertheless, this preference has slowly strengthened with time, as one would expect if it is indeed correct. Note that normal ordering alone does not presuppose a tiny effective mass; the smallest neutrino mass can still be sizable, as normal ordering does not necessitate normal hierarchy. Bayesian inference can be exploited to quantify the preference for mass ordering by considering the cosmological and neutrino oscillation constraints imposed on the available data . The results depend strongly on the choices of the prior (linear or logarithmic) and the parameter space (neutrino masses, or the smallest mass and mass-squared differences, or
and mass-squared differences, etc.). Normal ordering is most strongly preferred when the sampling is performed for the three neutrino masses with logarithmic priors . Insights can be gained by using oscillation and cosmology data to obtain the probability distribution formββ , from which the discovery potential of future experiments can be inferred . Figure 2 shows the Bayesian discovery probability, which corresponds to the chance of measuring a signal with a significance greater than or equal to 3σ. The bands are due to different assumptions in the NMEs. One can draw optimistic conclusions from these Bayesian studies. There is a better than-50% discovery probability for normal ordering and almost unity for inverted ordering for some of the future experiments. Beyond SM neutrino physics, the presence of light sterile neutrinos—prompted by LSND, MiniBooNE, short-baseline experiments, and other anomalies—can change the picture dramatically. The additional contribution to the effective mass from sterile neutrinos, |Ue4| 2 m4 |Ue4| 2 m2 41,is of the same order of magnitude as the minimal value of the effective mass in the inverted ordering of active neutrinos. It shifts the half-life distribution toward lower values (34); for normal ordering, the shift is toward larger values. The current situation on light sterile

neutrinos is confusing (35); most likely, not all hints are correct. Interestingly, the additional sterile-neutrino parameters that enter the effective mass are the same ones that could be responsible for the hints of active-to-sterile oscillation in reactor antineutrinos, for which extensive experimental efforts are being committed.

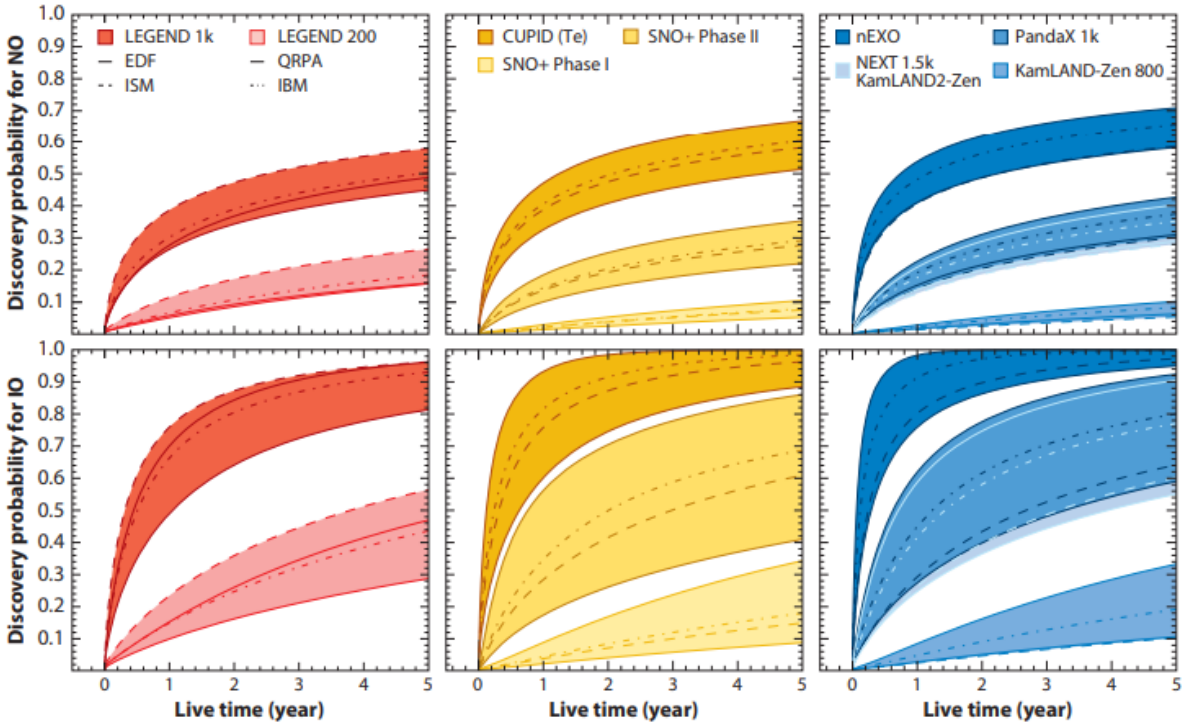

Fig3: Bayesian discovery probability for future experimental programs (CUPID, KamLAND-Zen, LEGEND, nEXO, NEXT, PandaX, SNO+) as a function of running time. The upper (lower) plots are for the normal (inverted) ordering. Abbreviations: EDF, energy-density functional; IBM, interacting boson model; ISM, interacting shell model; QRPA, quasiparticle random-phase approximation.

4.3 Alternative Mechanisms for Neutrinoless Double-Beta Decay

In the light-neutrino mechanism discussed so far, 0νββ-decay searches are directly testing light physics. Most alternative mechanisms are short-range mechanisms.3 If the light neutrino were replaced by a heavy neutrino (i.e., with a mass Mν larger than the 0νββ scale of |q| = 100 MeV), the propagator would become:

$$\frac{M_\nu}{M_\nu^2 - q^2} \simeq \frac{1}{M_\nu} \ll \frac{1}{\sqrt{|q^2|}}.$$

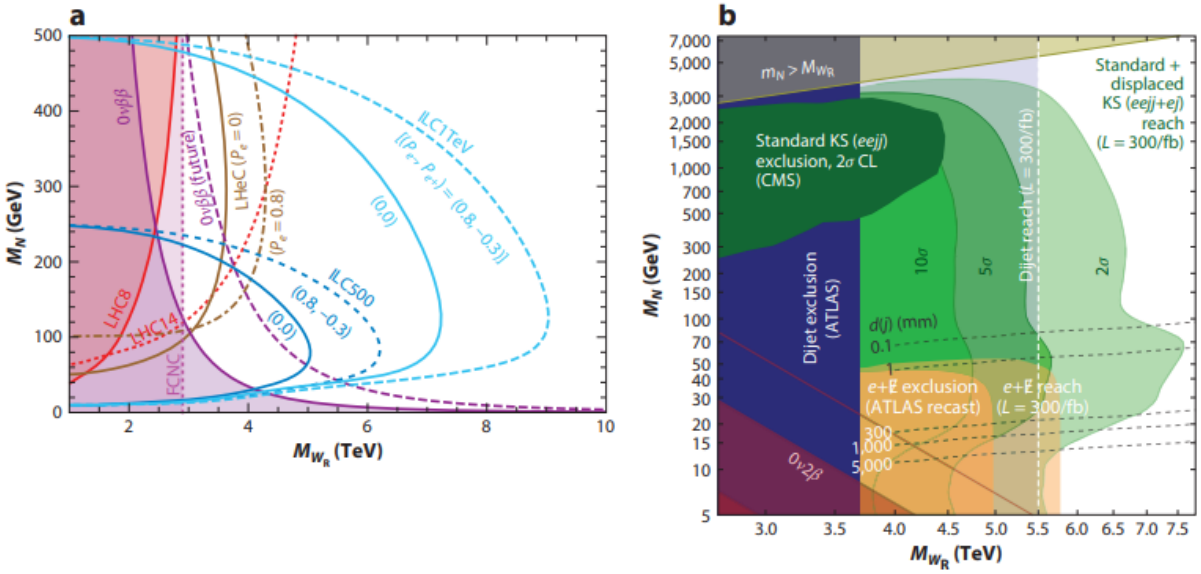

Fig4: Several examples of constraining and testing alternative 0νββ-decay mechanisms. (a) A comparison between various projected limits from future collider experiments on the right-handed neutrino and gauge boson mass. (b) The effects of displaced-vertex analysis on the same parameters. Abbreviations: FCNC, flavor-changing neutral current; ILC, International Linear Collider; KS, Keung–Senjanovic;´ LHC, Large Hadron Collider; LHeC, Large Hadron Electron Collider.

In fact, if only heavy particles mediate the decay, the amplitude of the process would be $A_{heavy} \sim c/M^5 = (c/M)^5$, where the mass scale M^5 is generally a combination of different particle masses. The corresponding amplitude for the standard one is $A_{st} \sim G^2 F m_{\beta\beta} /q^2$. The current limit of $m_{\beta\beta}$ yields $A_{st} \sim (0.3 \text{ TeV})^{-5}$, demonstrating that lepton-number-violating TeV-scale physics would generate 0νββ-decay half-lives corresponding to the current limits. This simple but illustrative and reasonably accurate estimate is the basis of many works on testing alternative 0νββ-decay diagrams with the same-sign dilepton processes pp → ee jj at the LHC, or similar processes at other colliders. By modifying Equation, we can express the half-life for heavy physics mechanisms very approximately (i.e., with much wider spread than the light-neutrino expression) as

$$T_{1/2}^{\text{heavy}} \sim 10^{27-28} \left(\frac{\tilde{c}/M}{\text{TeV}} \right)^{10} \text{years}.$$

A typical LHC test would work via the resonant production of a vector boson, and a Majorana fermion causes the subsequent lepton-number violation. The new particles in the 0νββ-decay diagram are not required to have the same or similar mass. The fermion could be much lighter than the vector boson, in which case the leptons and jets would be of low energy and would escape detection in the analysis. Displaced-vertex searches, such as those shown in Figure 4, are helpful in such instances. Future e+ e− or ep colliders have different characteristics in particle kinematics, allowing experiments to probe different areas in the parameter space. Moreover, the polarization of the initial-state fermions can help disentangle the chiral nature of the underlying process. Recent reviews on the tests of neutrino mass models and lepton-number violation at colliders can be found elsewhere.

As an example, there are left–right symmetric theories that contain heavy right-handed neutrinos NR and gauge bosons WR with mass MWR. Several diagrams for 0νββ decay arise in those theories , for instance, purely right-handed ones with NR and WR exchange, or mixed diagrams with light-neutrino exchange in which one of the currents is right-handed. The electrons in the latter diagrams are emitted with different helicities, which affect their angular distribution. The energy distribution of the individual electrons is

also different, which in principle would allow the driving mechanisms to be distinguished if the electrons can be tracked. Such an analysis has been performed in the SuperNEMO project .

A natural question to ask is whether 0νββ decay or collider limits will provide better constraints on the relevant model parameters. The answer depends on the various corrections that have not been studied for all mechanisms. As an example, a model with a Y = 1 SU(2)L doublet scalar and a singlet fermion. With various experimental and theoretical corrections included, it was shown that 0νββ decay would provide better reach in the search for TeV-scale lepton-number-violating interactions. The size of many theoretical corrections, however, is not completely understood and is a subject of debate. Nevertheless, LHC and 0νββ-decay searches are complementary approaches that provide a consistency check in case of a discovery.

Lepton-number violation observed at TeV scale has interesting cosmological implications. It is possible to translate an observed cross section of a lepton-number-violating process at the LHC into lepton-number-violating washout processes in the early Universe . Any lepton asymmetry generated by standard high-scale leptogenesis would typically be washed out, making this baryogenesis mechanism ineffective. With TeV-scale lepton-number violation, there is not really a need for standard high-scale leptogenesis; nevertheless, the interesting consequences of a TeV-scale observation of a 0νββ-like process are obvious. The black box, or Schechter–Valle, theorem states that any diagram causing 0νββ decay will generate a Majorana mass term for light neutrinos, rendering them Majorana particles. However, this is generally a mass term generated by a four-loop diagram that leads to a minuscule mass of the order of /($8\pi^2$) $4G^2$ Fm^6 q/mp 10^−29 eV, where we have used m_q = 5 MeV and 10^{-7}. In certain models, the connection of the 0νββ operator to a Majorana mass may be more direct. Examples are diagrams in which the particles that generate 0νββ decay are the same ones that generate the neutrino mass in one-loop mechanisms.
Finally, we note that several mechanisms for 0νββ decay may be present at the same time. They could even interfere with one another as long as the helicities of the emitted electrons allow for that.

4.4 QCD Corrections

QCD corrections to 0νββ-decay diagrams are important . Naïvely, the effect is of order αs/($16\pi^2$) log2/q2 0.1, where is the scale of the mechanism and q2 (100 MeV)^2 is the scale of the nuclear process. However, a Fierz transformation might be needed to generate a color-singlet final state that can be sandwiched between final-state nucleons. This procedure generates operators with different Lorentz structures, which can have drastically different NMEs, and so generates sizable corrections. The standard light-neutrino exchange diagram does not generate additional operators after applying the Fierz transformation to the QCD-corrected one; thus, it is not significantly affected by QCD corrections. Applying QCD corrections (as electroweak corrections are much smaller), the operators in the above equation are supposed to be run down to the scale of 0νββ decay of approximately 100 MeV. Below 1 GeV, the strong coupling becomes too large for applying perturbative techniques. There are ideas to cover this regime, but their numerical impact is not yet clear. QCD corrections to the long-range mechanisms are expected to be smaller than the NME uncertainties .

4.5 Alternative Processes

Over the years, there have been suggestions of other processes to probe low-energy lepton number violation, to identify the neutrino mass nature, or to entail both. The observation of these modes typically requires either non relativistic neutrinos or new interactions . For heavier neutrinos, the effects are observable only in certain mass ranges, such as in meson or W decays.

Neutrinoless double-electron capture , $(A, Z) + 2e^- \rightarrow (A, Z - 2)$, was of interest as an attractive alternative to $0\nu\beta\beta$ decay, since there was the possibility of a resonant enhancement if the initial- and final-state energies are close to degenerate . However, precise measurements of the involved nuclear masses disfavor this option. In addition, the decay to excited states, neutrinoless double-positron decay, or various combinations of electron capture and β or positron decay suffer from very low rates. Their observation would be a consistency check of the underlying mechanism of lepton-number violation and could provide useful information about the nuclear physics in neutrino-accompanied processes. $0\nu\beta\beta$ remains the most optimistic channel to answer the pressing questions of lepton-number violation and the neutrino nature

5.NUCLEAR AND HADRONIC PHYSICS ASPECTS

The NME for 0νββ decay can be written formally as,

$$\langle \text{final}|\mathcal{L}_{\ell-N}|\text{initial}\rangle.$$

What is needed for its evaluation are nuclear structure calculations for the final and initial nuclear states, as well as a proper transition from the fundamental lepton–quark Lagrangian to the lepton– nucleon one, L−N . Both problems are essentially independent of each other. Determining the accuracy and uncertainties of the various possible NMEs can be considered the most challenging theoretical problem that hinders precision studies of 0νββ decay in the event of a discovery.

5.1 Hadronization

While the fundamental 0νββ-decay Lagrangian is written at the quark level, hadrons are present in the nucleus. Moreover, operators need to be run from the fundamental high-lepton-number violating scale down to the nuclear scale, and then matched to the operators built from the hadronic degrees of freedom. A problem is that the hadronic operators are often phenomenologically written in terms of the form factors when the transition between quarks and nucleons is made, as in p|u¯(1 − γ5)d|n = e−i(p−p)xu¯(p)(FS(q2) + FPS(q2)γ5)u(p) ≡ JS−P. In this example, u(p) and u(p) are the spinors for the initial- and final-state neutron, and p − p = q. The q2 dependence of several form factors (particularly for scalar and pseudoscalar) is unknown, as is their normalization (particularly for tensors). The induced currents are also important, as one can see by considering the following nucleon matrix element that is particularly relevant for light-neutrino exchange:

$$\langle p|\bar{u}\gamma^{\mu}(1-\gamma_5)d|n\rangle \equiv J^{\mu}_{V-A}(x) = \bar{u}(p)\left(F_V(q^2)\gamma^{\mu} - iF_W(q^2)/(2m_p)\sigma^{\mu\nu}q_{\nu}\right.$$
$$\left. - F_A\gamma^{\mu}\gamma_5 + F_P(q^2)/(2m_p)\gamma_5 q_{\mu}\right)u(p')e^{iqx}\,.$$

The normalization factors Fi(q2 = 0) are the coupling constants; FV (q2 = 0) = gV and FA(q2 = 0) = gA are the vector and axial-vector coupling constants.

One can use the language of chiral symmetry and effective field theory to identify the necessary (i.e., the ones with the same symmetry structure under chiral symmetry) and leading hadronic operators. In chiral power counting, the ππ ee operator is the leading one, corresponding to a pseudoscalar interaction (two neutrons exchange a pion, which converts from a π− to a π+). There is an ongoing effort from the lattice QCD community to provide pion-level NMEs and the necessary low-energy coupling constants of the operators . In general, pion exchange implies a long-range interaction, which overcomes the usual suppression of the short-range diagrams. In mechanisms that induce pseudoscalar operators at the tree level, such as R-parity-violating SUSY, pion exchange can be expected to dominate. A general effective field theory framework that connects a chain of effective field theories through various scales, including those at lepton-number violation, electroweak-symmetry breaking, chiral symmetry breaking, and mπ , has recently been formulated

The induced pseudoscalar current that is proportional to FP in the above Equation is also connected to pion exchange. It has been argued that the correction to the leading Gamow–Teller matrix element is of the order q^2/(q^2 + m^2 π) ~ 30% in the light-neutrino case. The short-range contributions to the light-neutrino mechanism by using the chiral language mentioned above. Diagrams with ππ ee couplings generate ultraviolet divergences in the nn → pp ee amplitude, which can be cured by a counterterm in the form of a nucleon–nucleon contact term. Recent lattice calculations also identified a possibly important short-distance contribution . While leading in chiral power counting, its size is currently not determined well, and its impact is not clear.

5.2 General Aspects of the Nuclear Matrix Elements

Focusing on the most-referenced light-neutrino mechanism, we consider the quark-level current Jμ = u¯γ μ(1 − γ5)d. As a second-order process, a time-ordered integration is needed:

$$\int d^4x\, d^4y\, \langle f|T\{J^{\mu}(x)J^{\nu}(y)\}|i\rangle \propto \sum_n \frac{\langle f|J^{\mu}(\vec{q})|n\rangle\, \langle n|J^{\nu}(-\vec{q})|i\rangle}{|\vec{q}|(E_n + |\vec{q}| + E_{e2} - E_i)} + (e2 \to e1, \mu \leftrightarrow \nu),$$

which implies the introduction of a complete set of intermediate states of energy En. All states up to approximately 100 MeV contribute.4 The impulse approximation for the nuclear current J μ V −A in Equation sums over the individual free-nucleon matrix elements; in other words, only one nucleon experiences the weak decay without interference from the surrounding nuclear medium. The form factors need to be properly expanded in a nonrelativistic form. Various other approximations would then lead to the general formula in the above Equation. The NME is

$$\mathcal{M} = \mathcal{M}_{\mathrm{GT}} - \frac{g_V^2}{g_A^2}\mathcal{M}_{\mathrm{F}} + \mathcal{M}_{\mathrm{T}},$$

where the Fermi matrix element MF depends on the integral over |q | of FV (q 2) in its non relativistic approximation, whereas the Gamow–Teller matrix element MGT depends on the corresponding integrals over linear combinations of FA,P,W (q 2) (see References 56 and 87 for the explicit expressions). The tensor matrix element MT can be neglected. As an example, the Gamow–Teller matrix element, which is the leading one, can be written as

$$\mathcal{M}_{\mathrm{GT}} = g_A^2 \frac{2R}{\pi} \int_0^{\infty} d|\vec{q}|\, |\vec{q}|\langle f| \sum_{a,b} \frac{j_0(|\vec{q}|r_{ab})\, h_{\mathrm{GT}}(|\vec{q}|\vec{\sigma}_a \cdot \vec{\sigma}_b)}{|\vec{q}| + \bar{E} - (E_i + E_f)/2} \tau_a^+ \tau_b^+ |i\rangle,$$

where R is the nuclear radius of 1.2A3 fm, j0 is the Bessel function, hGT is a combination of FA,P,W properly expanded, and r_{ab} is the distance between the two decaying nucleons. Short-range correlations may be important, particularly for short-range mechanisms. The repulsion at short distances can be phenomenologically described by the UCOM, Jastrow, Argonne, or Bonn potential, with which the operators in the NMEs are multiplied.

The difficulty of NME calculations is to know the initial- and final-state nuclear wave functions, a many-body problem that in practice allows no exact solution. Several approaches to the problem exist and have been summarized in recent reviews . Figure 5 depicts the status

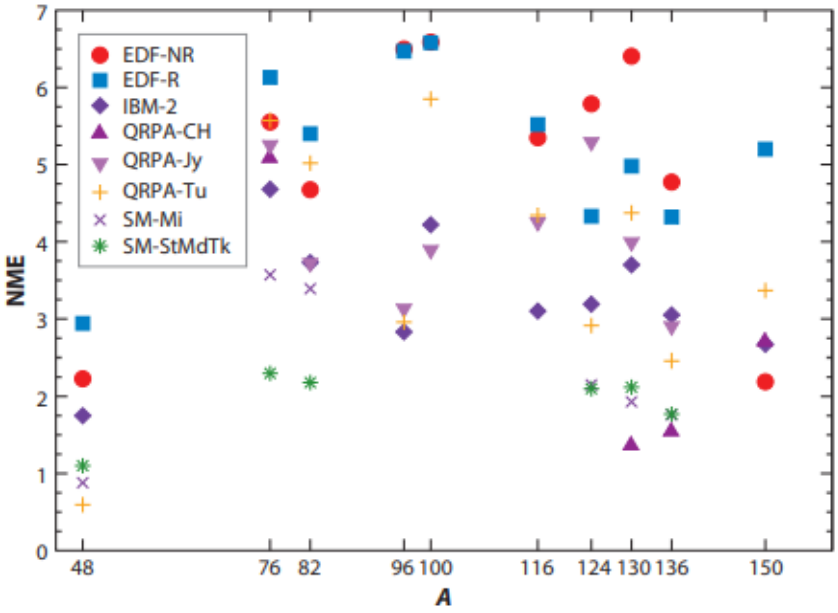

Fig 5: A representative compilation of nuclear matrix element calculations with an unquenched gA = 1.27 for different isotopes. Abbreviations: EDF, energy-density functional; IBM, interacting boson model; NME, nuclear matrix element; QRPA, quasiparticle random-phase approximation; SM, Standard Model.

of NME calculations for the different approaches. We summarize the main approaches in the remainder of this section.

The energy-density functional (EDF) and the generator coordinate methods (GCM) mix many mean fields with different properties , whereas the other methods use simple mean fields that the states and orbitals feel. Minimization of the energy functional finds the ground states. A large number of single-particle states are included and their collective motion is treated, but only a few selected correlations are used, possibly leading to an overestimation of the NME. The Projected Hartree–Fock–Bogoliubov Method (PHFB) is a related approach .

The nuclear shell model (NSM) does not use the full Hilbert space of the nucleon states, but only those in a valence space near the Fermi surface . The limited number of active nucleons and oscillator shells means that the low-lying states can be well described and reproduced, although the effects of pairing correlations may not be fully captured and may lead to an underestimation of the NME. Indeed, enlarging the configuration space would increase the matrix elements.

The interacting boson model (IBM) features nucleon pairs represented as bosons with certain quantum numbers and features a truncation of the full shell-model space to a subspace.More shells are used than in the NSM, but with fewer correlations . The description is typically more phenomenological than the other methods, and relies more on adjusting the model parameters to match the observables.

The quasiparticle random-phase approximation (QRPA) contains few correlations but a large number of single-particle orbits . The proton–neutron interaction quantified by a parameter g_{pp} should equal one in an exact calculation and diagonalization; it is fixed to a value that reproduces the measured 2νββ-decay half-lives. Also, the particle–hole coupling parameter can be fixed by observables.

The ab initio methods are a recent and promising line of development. All nucleons are taken as degrees of freedom, and interactions are fitted from the data involving nucleons or small nucleon systems. These approaches are currently limited by the availability of computing power. However, the recent results within the NSM for light isotopes and the 0νββ-decay candidate ^{48}Ca are encouraging .

All approaches miss certain features. Naïvely, one expects that the lack of configurations underestimates the NME, while the lack of correlations overestimates them, which is what the distribution in Figure 5 seems to confirm. There is hope that the calculations will converge as their respective shortcomings are overcome by future improvements.which discusses those attempts in detail.

The uncertainties in the NMEs are difficult to quantify. Some effects would shift all matrix elements, for example, the possible quenching of gA, while others are only applicable to certain models, such as the particle–particle coupling within QRPA. Although it is possible to study the effects by varying the nuclear model parameters , it is less clear how to quantify the shortcomings of the models in a systematic way. These desperately needed studies are under way as the associated uncertainties are expected to be larger than those from varying the model parameters. A multi-isotope 0νββ-decay program would surely help quantify and understand the current discrepancies.

5.3 Quenching

With the Gamow–Teller matrix element MGT the leading one in the light-neutrino exchange case, the NME is to a good approximation proportional to g2 A, and T0ν 1/2 is proportional to g^−4 A . Quenching denotes the reduction of gA that is necessary to reproduce the observable quantities of nuclear decays, particularly β and 2νββ decays. In addition, low-energy forward-angle charge-exchange reaction tests of the Ikeda sum rule confirm a reduced Gamow–Teller strength, as do the spectral measurements of

forbidden β decays . A reduced gA implies a longer T0ν 1/2, which is undesirable for experimental searches. Other alternative 0νββ-decay mechanisms would also be affected by quenching, though possibly to a lesser extent as MGT may not be the leading element.

The value of gA is used as an adjustment to bring observations in agreement with calculations. When the strength of the Gamow–Teller operator needs to be reduced, one reduces the axial coupling constant from its free nucleon value of 1.27. Possible origins of quenching are nuclear medium effects, many-body currents, or the inherent shortcomings of the nuclear many-body models. A possibly important observation is that β and 2νββ decays have energy scales of order MeV, that is, much smaller than the 0νββ scale of order 100 MeV. Low-energy processes may require more quenching as the missing particle–hole excitations in the models may shift the Gamow–Teller strength to higher energies. Thus, less or no quenching might be needed in 0νββ decay. However, conflicting statements in the literature exist. The dependence of quenching on the nuclear calculations can be demonstrated by analyzing the 2νββ electron-energy spectra, which allows the extraction of the subleading higher-order contributions to the matrix elements.

Non Nucleon degrees of freedom or many-nucleon currents may also shed light on the issue . In β and 2νββ decays, long-range pion exchange reduces the matrix elements significantly, whereas a reduction of only 10–30% was observed in 0νββ decay (as pion exchange contributes less at higher momenta). There are also indications that muon capture on nuclei requires less quenching, which again implies an energy dependence of the effect

In summary, recent studies indicate that there is less quenching necessary (not more than 20– 30%) in processes with large momentum transfer such as 0νββ decays. This reduction would correspond to an increase of T0ν 1/2 by a factor of approximately two to three. However, there is not yet consensus in the literature on this issue, and further experimental inputs and improvements in the calculations are desperately needed.

5.4 Experimental Tests of the Nuclear Matrix Elements

Hadronic charge-exchange reactions, whose transition matrix elements5 (related to the products of two β-decay Gamow–Teller matrix elements) can be accessed through reactions in the β− and β+ directions , provide a good test for the matrix elements in 2νββ decay. The neutrinoless mode and its NME problem can benefit from such nuclear structure measurements. For instance, the determination of the neutron occupancies in (p,t) two-nucleon transfer experiments has significantly influenced the QRPA calculations of the NMEs . One is normally interested in the Gamow–Teller operators, and has to choose reactions with small momentum transfer at the forward angles. With the proper choice of kinematics, charge-exchange reactions can also probe the transition strengths to the states beyond 1+. However, the hadronic operators do not exactly mimic 0νββ decay, and the crucial phases of the states are not accessible.

The NUMEN Collaboration recently presented a new approach. The goal is to use heavy-ion-induced double-charge-exchange reactions to test the second-order isospin response. Even at the forward angles, sizable momenta are transferred. Other similarities to 0νββ decay include complex nuclear medium effects and off-shell intermediate states of the reaction.6 The first measurements of the 40Ca(18O,18Ne)40Ar reaction were performed to demonstrate the experimental principle. Work is under way to probe reactions that involve the isotopes in 0νββdecay searches. Apart from various nuclear structure information, the quenching issue can also be addressed. The latter is also possible in muon-capture reactions

6.EXPERIMENTAL DESIGN CRITERIA

The observables in direct searches of 0νββ decay are the kinematic parameters of the two emitted electrons. A typical experiment measures the total energy (E) of the two electrons and may be able to reconstruct the individual electron paths (tracking) to reject backgrounds based on event topology. The observed 0νββ-decay signal is a monoenergetic peak at Qββ as there are no antineutrinos emitted in the decay. Since Qββ is well measured, usually in high-precision atomic traps, the signal search can be performed over a narrow energy window around Qββ ; the width of this region of interest (ROI) is selected on the basis of the energy resolution of the detector. The number of candidate events, N, observed in the ROI is

$$N = \ln(2)\frac{N_A}{W}\left(\frac{a\,\varepsilon\,Mt}{T_{1/2}^{0\nu}}\right),$$

where NA is Avogadro's number,W is the molar mass of the source, a is the isotopic abundance of the parent isotope, ε is the detection efficiency of the signal in the ROI, and t is the measurement time. The last factor of this expression captures the choices that an experimenter can make in designing an experiment.

The sensitivity to the half-life obviously would depend on the total number of counts in the ROI, some of which may be background events:

$$(T_{1/2}^{0\nu}) \propto \begin{cases} a\,M\,\varepsilon t & \text{background free,} \\ a\varepsilon\sqrt{\dfrac{Mt}{B\,\Delta E}} & \text{with background,} \end{cases}$$

where E is the detector energy resolution and B is the background index, normalized to the width of the ROI, source mass, and measurement time, for instance, in units of (keV·kg·year)−1. This expression clearly shows the advantage of a background-free experiment, as the T0ν 1/2 sensitivity would scale linearly with t as opposed to √t in the presence of backgrounds. In the following subsections, we discuss some of the design considerations in a 0νββ-decay experiment, including the choice of isotopes, sources of backgrounds, and their mitigation and elimination.

6.1 Isotope Choices

There are 35 isotopes capable of ββ decay , but not all of them are suitable as candidate isotopes for direct searches of 0νββ decays. Table 1 lists the characteristics of some of the isotopes that have been deployed in experiments. Given, an ideal isotope should have a high isotopic abundance (large a) and can be deployed in large quantities (large M) as high-resolution detectors (small E) under low-background conditions (small B). Unfortunately, such an isotope does not exist, and experimenters have to make design choices to optimize a subset of these parameters.

Table 1 Characteristics of commonly used $\beta\beta$-decay isotopes

Isotope	Natural abundance (%)[a]	$Q_{\beta\beta}$ (MeV)
^{48}Ca	0.187	4.263
^{76}Ge	7.8	2.039
^{82}Se	8.7	2.998
^{96}Zr	2.8	3.348
^{100}Mo	9.8	3.035
^{116}Cd	7.5	2.813
^{130}Te	34.08	2.527
^{136}Xe	8.9	2.459
^{150}Nd	5.6	3.371

The most critical consideration is the potential sources of backgrounds. An irreducible background to the 0νββ-decay search consists of the 2νββ-decay electrons; they are indistinguishable from those in the 0νββ-decay mode in the ROI. One way to mitigate this background is to deploy an isotope with a long 2νββ-decay half-life. The ratio of the 0νββ-decay signal to the 2νββ-decay background,

$$\frac{S}{B} \propto \left(\frac{Q_{\beta\beta}}{\Delta E}\right)^6 \frac{T_{1/2}^{2\nu}}{T_{1/2}^{0\nu}},$$

which indicates the importance of an excellent detector energy resolution for isotopes that have shorter 2νββ-decay half-lives

Primordial radioisotopes from the U and Th chains are ubiquitous in the detector construction materials. The most troublesome one is 208Tl. Its 2,615-keV γ -ray line lies above Qββ for a number of ββ-decay isotopes, and can deposit energy extraneously within the ROI. Another problematic background comes from 222Rn, whose progeny 214Bi emits a β electron with an energy up to 3,270 keV. An ideal 0νββ-decay isotope candidate would have a Qββ high enough to avoid these backgrounds.

The detection efficiency of the 0νββ-decay signal can be significantly enhanced if the source material is integrated as the detector medium. As the path lengths of the two signal electrons are much shorter than the size of the active medium in such a coalesced configuration, calorimetry with excellent energy resolution is possible. When the source material is external to the detector, the probability of at least one of the two electrons escaping detection or with degraded energy increases due to self-absorption. The main advantage of this external-source configuration is the possibility of superior tracking and effective background rejection, but at the expense of energy resolution.

To reduce the cost of an experiment, an ideal source material should be readily available in its natural form and the candidate isotope within it should have a high natural abundance. The cost of isotope enrichment typically depends on the isotopic abundance of the starting material—the higher the natural abundance, the lower the cost. If the natural abundance is high enough, isotope enrichment may be unnecessary, as has been demonstrated in the case of 130Te.

6.2 Backgrounds

The T0ν 1/2 discovery potential would shrink substantially in the scenario of a nonvanishing background index. For the next generation of experiments to reach a discovery potential of T0ν 1/2 ~ 10^28 years, an

extremely stringent background index of <0.1 count/(FWHM·tonne·year), where FWHM is the full width at half maximum of the detector resolution at Qββ , is necessary.

As discussed above, a careful choice of target isotope and detector technology could diminish the impact of the irreducible 2νββ-decay background on the discovery potential. Similarly for the omnipresent solar neutrinos, their impact can be mitigated by a high mass loading of the decaying isotope in the target medium to improve the ratio of the signal to the neutrino–electron elastic scattering background. This is particularly important for large (kilotonne-scale) liquid-scintillator detectors.

In 0νββ-decay experiments, several types of backgrounds can be controlled through careful design and vigilant implementation. Trace amounts of radioisotopes from the natural U and Th chains must be kept to a minimum in any materials close to active detector volume. Other pervasive natural radioactivities, such as 3H, 14C, and 40K, have lower decay energies and do not impinge on 0νββ-decay searches. The techniques to produce radio pure materials for mechanical support are constantly being explored and refined, for example, electroformed Cu and alloys and polymers. Radioassay results from prior generations of low-background experiments are now readily accessible as online databases to aid the material selection process for future experiments. Even when intrinsically radiopure construction materials have been identified, extreme care to maintain their cleanliness is essential. For example, exposure to 222Rn would result in increased α and β emitter backgrounds on the surface or in the bulk of the unprotected components

Natural radioactivities far away from the active detector volume, including γ -rays from the primordial chains and neutrons from (α, n) reactions originating from the rock wall of the underground laboratory, can be blocked by passive shielding with clean Pb or Cu, water, or liquid cryogen. The last two options may also allow the shielding medium to serve as an active veto to reject cosmic rays

Cosmic-ray muons (μ) can induce several types of background in a 0νββ-decay experiment. For experiments at deep underground laboratories, prompt muon interactions in the detectors do not usually pose any background concerns. These interactions typically deposit a large amount of energy and can be vetoed easily. The activation of long-lived isotopes and the production of secondary neutrons are the main worries.Muons can induce these backgrounds via different mechanisms: μ− capture in nuclei, muon–nucleon quasi-elastic scattering, electromagnetic showers, and photo-neutron production through virtual photon exchange. High-energy neutrons produced in inelastic neutron scattering (n, n γ) are also a source of background in 0νββ-decay experiments.

Numerous theoretical and experimental studies have been performed to determine the production yield of these radioisotopes after the materials that are commonly used in dark matter and ββ-decay searches have been exposed to cosmic rays at or above the Earth's surface. There are two strategies to mitigate these activated backgrounds: to minimize the exposure to cosmic rays on the surface and to let the materials cool down underground after such exposure. However, it would be impractical to wait for certain long-lived radioisotopes to decay to an acceptable activity.

The backgrounds from cosmogenic production of radioisotopes in situ during the experiment are difficult to identify, as their decays could occur long after the initial muons. Although this is an irreducible background, its impacts can be mitigated by simply deploying the experiment at a greater depth. This type of background is of particular concern to experiments in which the ββ-decay isotopes are dissolved in a large volume of host medium given the large mass and the broad energy spectrum of the activated products. Experiments with tracking or event position reconstruction capabilities can reject these backgrounds by temporal and spatial correlations.

6.3 Detection Strategies

As with any search for New Physics, the primary goal of the detector design is to discriminate between signal and backgrounds effectively while maintaining high signal detection efficiency. The most common way to achieve this discrimination is via energy resolution, which is generally intrinsic to the detection medium. For the next generation of experiments, it will also be essential to maximize the discovery potential. This means actively showing that any observed signal is not only consistent with the expected 0νββ-decay signal but also inconsistent with the measured backgrounds.

0νββ has a characteristic event topology with the emission of two ~MeV electrons. Low Density-gas tracking detectors can in principle resolve the two electron tracks, leaving only the irreducible background from 2νββ decay. For detectors with higher density, such as discrete detectors or liquid-scintillator detectors, these electrons deposit their energy within a few millimeters, allowing a less powerful but still useful discrimination between compact signal-like events and γ -rays, which are likely to scatter and deposit energy at multiple sites. The difference may be resolved through discriminating between the so-called single-site and multisite events by pulse shape discrimination or reconstructed event topology, depending on the position resolution, as well as the size and type of a given detector. Some detectors are capable of particle discrimination through multiple detection channels, such as scintillation and ionization, which could allow for the identification of α backgrounds.

Timing is yet another key variable for distinguishing signals from backgrounds. For example, in the aforementioned 222Rn chain, the particularly troublesome 214Bi progeny decays in coincidence with 214Po α decay, which has a 160-μs half-life. For some detectors, this timing coincidence can be used to identify 214Bi decays both in the bulk material and on the surfaces.

The spatial distribution of background events can be quite different from that of the signal events. The 0νββ-decay events will be uniformly distributed throughout the source material, as will background events from 2νββ decay and other uniformly distributed radioactive sources. However, additional backgrounds will come from the mechanical support materials and localized detector components. Background events will be concentrated close to those inactive materials. In experiments with discrete detectors, each detector may serve as a veto for other detectors in the system; multiple-scattered background γ -rays or βγ decays are likely to deposit energy in more than one detector. In monolithic detectors, these background events may be rejected by an optimized fiducial volume cut. This configuration also enables the measurement of these backgrounds with high statistics, which can in turn be used as a constraint in the 0νββ-decay analysis.

Many experiments use multiple variables to distinguish between signal and backgrounds.While this can be accomplished with hard cuts or a multidimensional fit, another option is to create an optimized discriminator variable based on machine learning techniques. In future searches, deep learning methods may also be applied to the problem of signal-to-background optimization
Another technique that can distinguish 0νββ decay from all backgrounds other than 2νββ decay is the identification of the decay daughter on an event-by-event basis. The prototypical isotope for this technique is 136Xe (152). The ββ decay of 136Xe results in an ionized Ba daughter. This has been an intriguing system, with efforts by both the nEXO and NEXT Collaborations to identify single Ba ions with high efficiency. This technique still presents significant challenges to implementation, but the implications for positive identification of a ββ decay and the background rejection capabilities are significant enough to motivate continued development for deployment in future experiments.

Table 2 $T^{0\nu}_{1/2}$ and $\langle m_{\beta\beta}\rangle$ limits (90% CL) from the most recent measurements, sorted by mass number

Isotope	$T^{0\nu}_{1/2}$ ($\times 10^{25}$ years)	$\langle m_{\beta\beta}\rangle$ (eV)	Experiment	Reference
^{48}Ca	$>5.8 \times 10^{-3}$	<3.5–22	ELEGANT-IV	159
^{76}Ge	>8.0	<0.12–0.26	GERDA	160
	>1.9	<0.24–0.52	Majorana Demonstrator	161
^{82}Se	$>3.6 \times 10^{-2}$	<0.89–2.43	NEMO-3	162
^{96}Zr	$>9.2 \times 10^{-4}$	<7.2–19.5	NEMO-3	163
^{100}Mo	$>1.1 \times 10^{-1}$	<0.33–0.62	NEMO-3	164
^{116}Cd	$>2.2 \times 10^{-2}$	<1.0–1.7	Aurora	165
^{128}Te	$>1.1 \times 10^{-2}$	NE	C. Arnaboldi et al.	166
^{130}Te	>1.5	<0.11–0.52	CUORE	126
^{136}Xe	>10.7	<0.061–0.165	KamLAND-Zen	167
	>1.8	<0.15–0.40	EXO-200	168
^{150}Nd	$>2.0 \times 10^{-3}$	<1.6–5.3	NEMO-3	169

The $\langle m_{\beta\beta}\rangle$ limits are listed as reported in refereed publications. Other unpublished preliminary results are described in the text. Abbreviation: NE, not evaluated.

7.EXPERIMENTAL CHALLENGES AND STRATEGIES

In the standard interpretation of neutrinoless double-beta decay in terms of mass mechanism, experimentalists designing a neutrinoless double-beta decay experiment have three hurdles to leap over in front of them. The first consists in scrutinizing the much debated 76Ge: recent experimental results and present developments are very close to accomplishing this task. The second one consists in approaching and then covering the inverted hierarchy region of the neutrino mass pattern. The third and ultimate goal is to explore the direct hierarchy region. In this section, we discuss the main guidelines to achieve these targets.

7.1 Size of the Challenge

First, we have to quantify in terms of signal and background rates the challenges that the experimentalists have to cope with. Since we do not want to be precise here, but just to assess orders of magnitude, we will make crude approximations in the formula of 3.5 which gives the rate. We will take M0ν ≈ 3.5 for the nuclear matrix elements this choice is motivated by the results discussed in Section 5 and shown in Figure 7. We observe then that for most of the experimentally relevant isotopes the phase space term G01 including the factor g4 A with the axial coupling constant gA set equal to 1.25 is in the range 2 × 10−13 − −5 × 10−14 y−1 with significant exceptions discussed in Section 6.2. We will therefore consider a sort of "average" candidate isotope with M0ν 3.5 and G01 4 × 10−14 y−1. In Table 3, we report the rates for 1 kmol of isotope for this standard candidate in correspondence with the reference values of <mv>.

Table 3: Signal rates for an "average" double-beta decay candidate.

$\langle m_\nu \rangle$ (meV)	Signal rate (counts/(y kmol))	Significance of $\langle m_\nu \rangle$ value
300	~70	^{76}Ge claim in the Heidelberg-Moscow experiment
50	~2	Higher bound of the inverted hierarchy region
20	~0.2	Lower bound of the inverted hierarchy region
3	$\sim 7 \times 10^{-3}$	Center of the direct hierarchy region

Considering that 1 kmol corresponds typically to several tens—one hundred kilograms of isotope mass, and that it is meaningful to operate a well designed 0νββ experiment for ~5 y, we immediately see that while scrutinizing the 76Ge claim may be done in principle with only ~10 kg isotope, we need typically 1 ton of isotope mass in order to explore the inverted hierarchy region, just to accumulate a few signal counts. The direct hierarchy region seems for the moment out of the reach of the present technologies, since one would need sources of the order of 1 Mmol typically 100 tons.

In addition, in order to appreciate such tiny signal rates, the background needs to be extremely low. The experimentalists are obliged to operate in conditions of almost zero background, given the constraints imposed by the size of the source. Acceptable background rates are of the order of 1–10 counts/y kmol if the goal is just to approach or touch the inverted hierarchy region, whereas one needs at least one order of magnitude lower values to explore it fully, around or even less than 1 count/y ton.

7.2 Choice of the Double-Beta Decay Isotope

Which are the best isotopes to search for neutrinoless double-beta decay? Experimental practice shows that the following three factors weight the most in the design of an experiment:

- i the Q-value,
- ii the isotopic abundance together with the ease of enrichment,

- iii the compatibility with an appropriate detection technique.

The Q-value is probably the most important criterion. It influences both the phase space and the background. It is essentially a Q-value-based selection which determines the fact that at the moment there are only 9 experimentally relevant isotopes listed in Table 4, which also reports other parameters and notes relevant for the discussion in the present section. The Q-values of all these isotopes are larger than 2.4 MeV, with the important exception of 76Ge Q-value 2.039 MeV which remains in the elite mainly thanks to factor iii. One can get a grasp of the Q-value situation in Figure 8, where all the 35 double beta unstable nuclei are reported with their energy transition. The "magnificent nine" are highlighted. Two markers indicate two important energy limits in terms of background: the 2615 keV line represents the end-point of the natural gamma radioactivity; the 3270 keV line represents the Q-value of the 214Bi beta decay, which, among the 222Rn daughters, is the one releasing the highest-energy betas and gammas. The 9 candidates are divided by these two markers in three groups of three isotopes. The first group 76Ge, 130Te, and 136Xe has to cope with some gamma background and with the Radon-induced one; the second group 82Se, 100Mo, and 116Cd is out of the reach of the bulk of the gamma environmental background but Radon may be a problem; the candidates of the third group 48Ca, 96Zr, and 150Nd are in the best position to realize a background-free experiment. As for the phase space, the situation is depicted in Figure 9. No great differences are observable among the various candidates, with the significant exceptions of 76Ge, which presents a small value of only ~ 6 × 10−15 y−1 due to its low Q and, on the other side of 150Nd, characterized by a particularly high value of ~ 1.5 × 10−13 y−1.

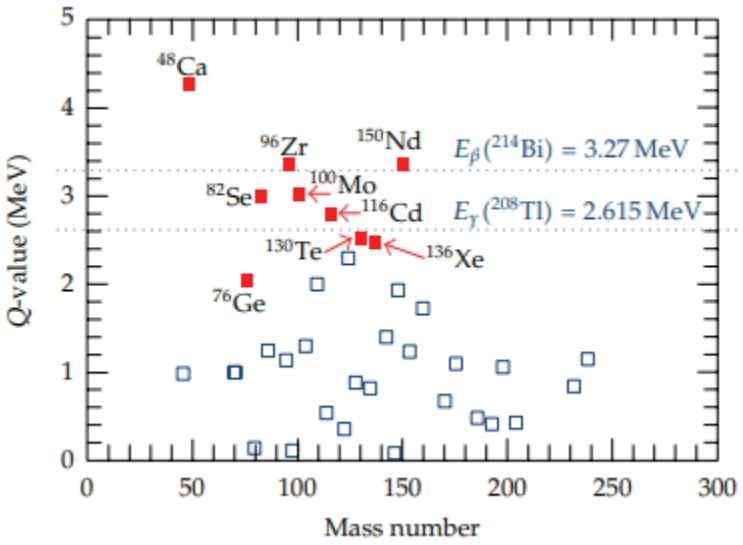

Fig6: Double-beta decay candidates and their Q-values. The "magnificent nine" are highlighted and two background-relevant energy markers are indicated

Table 4: Relevant parameters and features of the "magnificent nine" double-beta decay candidates.

Double-beta candidate	Q-value (MeV)	Phase space G_{01} (y^{-1})	Isotopic abundance (%)	Enrichable by centrifugation	Indicative cost normalized to Ge
^{48}Ca	4.27226 (404)	6.05×10^{-14}	0.187	No	—
^{76}Ge	2.03904 (16)	5.77×10^{-15}	7.8	Yes	1
^{82}Se	2.99512 (201)	2.48×10^{-14}	9.2	Yes	1
^{96}Zr	3.35037 (289)	5.02×10^{-14}	2.8	No	—
^{100}Mo	3.03440 (17)	3.89×10^{-14}	9.6	Yes	1
^{116}Cd	2.81350 (13)	4.08×10^{-14}	7.5	Yes	3
^{130}Te	2.52697 (23)	3.47×10^{-14}	33.8	Yes	0.2
^{136}Xe	2.45783 (37)	3.56×10^{-14}	8.9	Yes	0.1
^{150}Nd	3.37138 (20)	1.54×10^{-13}	5.6	No	—

As for the second criterion, natural isotopic abundances are reported in Table 4. Most of the abundances are in the few % range, with two significant exceptions: the positive case of 130Te that with its 33.8% value can be studied with high sensitivities even with natural samples; the negative case of 48Ca, well below 1%. Given the considerations exposed in Section 6.1, an ambitious experiment aiming at exploring the inverted hierarchy region of the neutrino mass pattern needs at least 100 kg of isotope mass. In order to keep the detector size reasonable and recalling that the background scales roughly as the total source, and not isotope, mass, it is clear that isotopic enrichment is a necessary task for almost all high sensitivity searches. The generally available enrichment techniques are reported in Table 5.

Table 5: Existing methods for isotope separation. The technologies relevant for neutrinoless double-beta decay are indicated in the fourth and in the three last lines.

Method of separation	Energy (eV/atom)	Status	Production capacity	Scale of price	Special requirements
Electromagnetic	10^6–10^7	Commercial	~100 g/y	High	—
Gas diffusion	3×10^6	Industrial	>tons/y	Medium	Gas compound
Gas nozzle	10^6	Industrial	>tons/y	Medium	Gas compound
Gas centrifuge	3×10^5	Industrial	>tons/y	Low	Gas compound
Rectification	10^2	Industrial	>tons/y	Low	Light elements
Isotope exchange	10^2	Industrial	>tons/y	Low	Light elements
Ion cyclotron resonance	10^3	R&D	~100 kg/y	Medium	—
Atomic vapor laser I.S.	10^2	R&D	>100 kg/y	Medium	—
Molecular laser I.S.	10^2	R&D	>100 kg/y	Medium	—

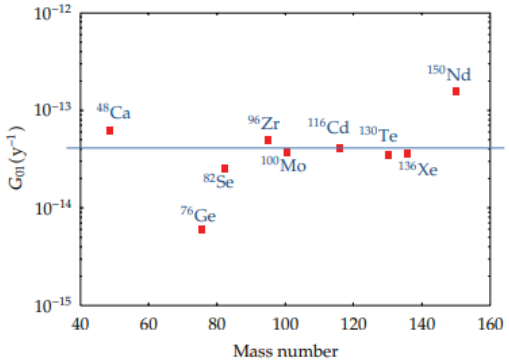

Fig7: Phase space of the nine more favorable double-beta decay isotopes values taken and multiplied by g4 A with the axial coupling constant gA set at 1.25. The line refers to the "average" candidate considered in Section 7.1.

The role of the third criterion will become more clear in the following sections, where specific detection technologies will be described. We would like however to discuss here three special emblematic cases in which the detector principle matches favorably with the isotope to study.

- i 76Ge large volume, high-purity, and high-energy resolution Ge-diodes are currently employed in gamma spectroscopy. A detector of this type containing germanium enriched in 76Ge is almost ideal for double-beta decay search. This explains why past Heidelberg-Moscow and IGEX and present GERDA and Majorana experiments were and are at the forefront in the field, in spite of the relatively low Q of this isotope.
- ii 130Te large crystals up to 1 kg of the compound TeO2 can be grown with high radiopurity. They can be used for the realization of bolometers with excellent performance. Given also the high natural isotopic abundance of 130Te, it is understandable why a past experiment like

Cuoricino has been leading the field for several years, and why CUORE is one of the most promising future searches both are based on arrays of TeO2 bolometers.

- iii 136Xe liquid and gaseous xenon is an ideal medium for particle detection. It can be used to equip TPCs with tracking/topology capability. Scintillation and ionization can provide reasonable energy resolution. This approach is exploited in experiments like EXO now leading the field and NEXT. In addition, xenon can be easily dissolved in organic liquid scintillators, allowing it to reach very large masses exploiting existing facilities; this is the case of KamLAND-Zen. Last but not least, xenon is the element that can be isotopically enriched at the lowest prices and with the highest production capacity.

For the usual conspiracy of Nature, the three mentioned isotopes are the least favorable among the "magnificent nine" in terms of Q-value, but nevertheless they provide at the moment the most stringent limits on neutrinoless double-beta decay. This fact explains better than any digression how the detection technique remains a crucial factor for a highly sensitive search.

7.3 Experimental Approaches and Methods

From the experimental point of view, the shape of the two-electron sum energy spectrum enables to distinguish among the two discussed decay modes. In case of 2νββ, this spectrum is expected to be a continuum between 0 and Q with a maximum around 1/3 · Q. For 0νββ, the spectrum is just a peak at the energy Q, enlarged only by the finite energy resolution of the detector. The two distinctive energy distributions are shown in Figure 10a. Additional signatures for the various processes are the single-electron energy distribution and the angular correlation between the two emitted electrons. As we have previously discussed, Q ranges from 2 to 3 MeV for the most promising candidates.
The experimental strategy pursued to investigate the 0νββ decay consists of the development of a proper nuclear detector, with the purpose to reveal the two emitted electrons in real time and to collect their sum energy spectrum as a minimal information. Additional pieces of information can be provided in some cases, like single-electron energy and initial momentum, or, in one proposed approach, the species of the daughter nucleus. The desirable features of this nuclear detector are as follows.

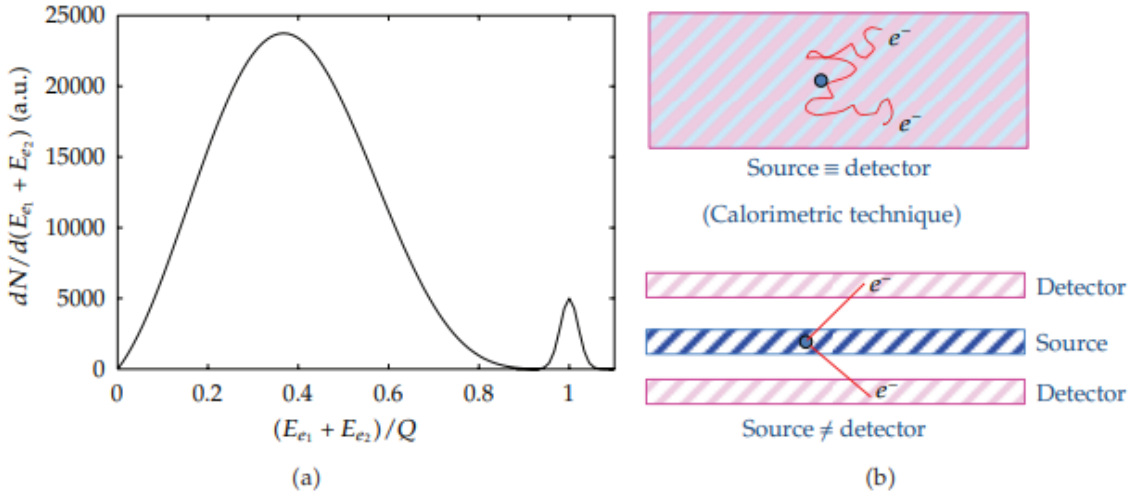

Fig8: : a Distribution of the sum of the two electron energies for 0νββ and 2νββ, obtained assuming that the 2νββ rate is 100 times faster than the 0νββ, and the FWHM detector energy resolution is 5%. b Schematic representation of the calorimetric technique and of the external source approach.

- i High-energy resolution, since a peak must be identified over an almost flat background in case of 0νββ. In particular, this feature is very useful to keep under control the background induced by

the tail of the 2νββ spectrum. It can be shown that the ratio R0ν/2ν of counts due to 0νββ decay over those due to 2νββ in a narrow window around the Q-value

$$R_{0\nu/2\nu} = \frac{m_e}{7Q\delta^6} \frac{T_{1/2}^{2\nu\beta\beta}}{T_{1/2}^{0\nu\beta\beta}},$$

\where δ ΔEFWHM/Q is the fractional energy resolution at the Q-value. It is worth to note the strong dependence on the energy resolution of this expression. Candidates with a slow 2νββ decay rate like 136Xe, for which T2νββ 1/2 2.2 × 1021 y are of course more favorable than those with a fast 2ν process like 100Mo, for which T2νββ 1/2 7.1 × 1018 y. For the latter ones, an excellent energy resolution <1% is mandatory

- ii Low background, which requires underground detector operation to shield cosmic rays, very radiopure materials the competing natural radioactivity decays have typical lifetimes of the order of 109 , 1010 years versus lifetimes longer than 10^25 years for 0νββ, and well-designed passive and/or active shielding against local environmental radioactivity.
- iii Large source, in order to monitor many candidate nuclides. Present sources are of the order of 10–100 kg in the most sensitive detectors, while experiments capable of covering the inverted hierarchy region need sources in the 100–1000 kg scale.
- iv Tracking and topology capability for the nuclear events, useful to reject background and to provide additional kinematical information on the emitted electrons.

Normally, the listed features cannot be met simultaneously in a single detection method. It is up to the experimentalist to choose the philosophy of the experiment and to select consequently the detector characteristics, privileging some properties with respect to others, having in mind of course the final sensitivity of the setup to half-life and to mν.

The searches for 0νββ can be further classified into two main categories: the socalled calorimetric technique, in which the source is embedded in the detector itself, and the external-source approach, in which source and detector are two separate systems.

The calorimetric technique has been proposed and implemented with various types of detectors, such as scintillators, bolometers , solid-state devices, and gaseous chambers. There are advantages and limitations in this technique, which are here summarized:

- due to the intrinsically high efficiency of the method, large source masses are possible: ~100 kg has been demonstrated; ~1000 kg is possible;
- with a proper choice of the detector type, a very high energy resolution of the order of 0.1% is achievable, as in Ge-diodes or in bolometers;
- there are severe constraints on detector material and therefore on the nuclides that can be investigated;
- it is difficult to reconstruct event topology, with the exception of liquid or gaseous Xe TPC, but at the price of a lower energy resolution.

For the external-source approach, many different detection techniques have been experimented as well: scintillation, gaseous TPCs, gaseous drift chambers, magnetic field for momentum and charge sign measurement, and time of flight. These are the main features, with positive and negative valence:

- A neat event reconstruction is possible, making easier the achievement of a virtual zero background: however, 0νββ cannot be distinguished by 2νββ event by event if the total electron

energy is around Q; therefore, because of the low energy resolution, 2νββ constitutes a severe background source for 0νββ.

- Large source masses are not easy to achieve because of self-absorption in the source, so that the present limit is around 10 kg; 100 kg is possible with an extraordinary effort, while 1000 kg looks out of the reach of this approach.
- Normally the energy resolution is low of the order of 10%, intrinsically limited by the fluctuations of the energy that the electrons deposit in the source itself.
- Efficiency is also low in prospect of the order of 30%.

7.4 The Experimental Sensitivity

In order to compare different experiments, it is useful to give an expression providing the sensitivity of an experimental setup to the 0νββ lifetime of the investigated candidate, and hence to determine the sensitivity to mν in case of mass mechanism. The first step involves only detector and setup parameters, while for the second step one needs reliable calculations of the NMEs, extensively discussed in Section 4. The sensitivity to lifetime F can be defined as the lifetime corresponding to the minimum detectable number of events over background at a 1 σ confidence level. For the case of a source embedded in the detector and nonzero background, it holds

$$F = \frac{N_A \cdot \varepsilon \cdot \eta}{A} \cdot \left(\frac{M \cdot T}{b \cdot \Delta E} \right)^{1/2},$$

where NA is the Avogadro number, M is the detector mass or source mass, in case of external-source approach, ε is the detector efficiency, η is the ratio between the total mass of the candidate nuclides and the detector source mass, ΔE is the energy resolution, and b is the specific background, for example, the number of spurious counts per mass, time, and energy unit.

From this formula, one can see that in order to improve the performance of a given set-up, one can use either brute force e.g., increasing the exposition M · T or better technology, improving detector performance ΔE and background control b. Next Generation experiments require work on both fronts.

8. EXPERIMENTAL SITUATION

8.1 Past Experiments

In the nineties of the last century, the double-beta decay scene was dominated by the Heidelberg-Moscow HM experiment. This search was based on a set of five Ge-diodes, enriched in the candidate isotope 76Ge at 86%, and operated underground with high energy resolution typically, 4 keV FWHM in the Laboratori Nazionali del Gran Sasso LNGS, Italy. This search can be considered, even from the historical point of view, as the paradigm of the calorimetric approach. The total mass of the detectors was 10.9 kg, corresponding to a source strength of 7.6 × 1025 76Ge nuclei. The raw background, impressively low, is 0.17 counts/kev kg y around Q 2039 keV. It can be reduced by a further factor 5 using pulse shape analysis to reject multisite events. The limits on halflife and mν are, respectively, 1.9 × 1025 y and 0.3–0.6 eV depending on the NMEs chosen for the analysis. A subset of the HM collaboration has however claimed the discovery of 0ν2β decay in 2001, with a half-life best value of 1.5 × 1025 y 0.8 − 18.3 × 1025 y at 95% c.l., corresponding to a best value for mν of 0.39 eV 0.05 − 0.84 eV at 95% c.l. including nuclear matrix element uncertainty 59. This claim is based on the identification of tiny peaks in the region of the 0ν2β decay, one of which occurs at the 76Ge Q-value. However, this announcement raised skepticism in the double-beta decay community 60, including a part of the HM collaboration itself, due to the fact that not all the claimed peaks could be identified and that the statistical significance of the peak looked weaker than the claimed 2.2 σ and dependent on the spectral window chosen for the analysis. However, new papers 8, 64 published later gave more convincing supports to the claim. The quality of the data treatment improved, and the exposure increased to 71.7 kg·y. In addition, a detailed analysis based on pulse shape analysis suggests that the peak at the 76Ge Q-value is mainly formed by single-site events, as expected in case of double-beta decay, while the nearby recognized γ peaks are compatible with multisite events, as expected from γ interaction in that energy region and for detectors of that volume. A 4.2 σ effect is claimed. The half-life value claimed in the last paper is 2.3 × 10^25 yr. The HM experiment is now over, and the final word on this crucial result will be given by other searches.

The top level of the external-source technique was reached nowadays by the NEMO3 experiment. The NEMO3 detector, installed underground in the Laboratoire Souterrain de Modane LSM, in France, is based on well-established technologies in experimental particle physics: the electrons emitted by the sources cross a magnetized tracking volume instrumented with Geiger cells and deliver their energy to a calorimeter based on plastic scintillators. Thanks to the division in 20 sectors of the set-up, many nuclides can be studied simultaneously, such as 100Mo, 82Se, 150Nd, 116Cd, 130Te, 96Zr, and 48Ca. The strongest source was 100Mo with 4.1 × 1025 nuclei. The energy resolution ranged from 11% to 14.5%. Results achieved with 100Mo fix the half-life limit to 1 × 1024 y, corresponding to limits of 0.8–1.3 eV on mν. In the NEMO3 experiment, all the bonuses and all the limits of the external-source approach show off. From one side, the NEMO3 detector produces beautiful reconstruction of the sum and single-electron energy spectrum, and precious information about the angular distribution. Double-beta decay events can be neatly reconstructed with excellent background rejection. Thanks to the multisource approach, 2ν2β decay has been detected in all the seven candidates under observation, a superb physical and technical achievement which makes the NEMO3 set-up a real “double-beta factory.” On the other hand, the low energy resolution and the unavoidable “bidimensional” structure of the sources make a further improvement of the sensitivity to 0ν2β quite difficult, because of the background from 2ν2β and the intrinsic limits in the source strength.

8.2 Results of recent Experiments

Table 6 presents the results of experiments on the search for 0νββ decay, as well as the main parameters of the installations used. It can be seen that eight different isotopes were studied using completely different techniques and detectors. The measurement statistics are also different, from 0.12 kg·yr in the CANDLES-III experiment to 970 kg·yr in the KamLAND-Zen experiment. An important parameter is the

energy resolution of the detectors (FWHM) in the region of Qββ. The best energy resolution was achieved in the Majorana Demonstrator experiment with HPGe detectors (2.52 keV), while the worst was found in the NEMO-3 and KamLAND-Zen experiments (~250 keV). One of the most important parameters of such installations is the background index (BI) in the energy range of 0νββ decay and the background index multiplied by the energy resolution (BI·FWHM). The lowest background index was obtained in the KamLANDZen experiment (~7 × 10−5 c/keV·kg·yr), but the best BI·FWHM value (which is much more important) was obtained in the GERDA experiment (~1.8 × 10−3 c/kg·yr). The limits presented in Table 1 are the best to date and define the state of the research in 0νββ decay. In the experiments with the best sensitivity (KamLAND-Zen and GERDA), a limit on the half-life of ~2 × 1026 years was achieved; in three experiments [25,28,29], limits of ~(2–8) × 1025 years were attained; and in other three experiments [30–32], limits of ~(2–4) × 1024 years were obtained (all limits at 90% C.L.). The limits on hmvi are given in the seventh column of Table 6 (these are the values given by the authors in the relevant publications). It can be seen that in all cases, we are dealing with a fairly wide range of values. This is due to uncertainties in the NME calculations. Still, more conservative values seem to be more realistic (closer to the right boundary of the interval), and it is on them that one should reply when planning new experiments. From the obtained results, we can conservatively conclude that the current limit on hmvi is ~0.16 eV (90% C.L.). The current state of the problem of NME calculations can be found in. Only three experiments from Table 1 are still active today: these are KamLAND-Zen, CUORE, and CANDLES-III. It can be expected that in a few years, new, several times more stringent limits on T1/2 for 136Xe, 130Te, and 48Ca will be obtained. In addition, in 2023, LEGEND-200 started the data taking. Using the data of oscillatory experiments, one can obtain predictions for possible values of hmνi. Usually, a so-called "lobster" plot is constructed, which shows the possible values of hmνi, depending on the type of ordering and the mass of the lightest neutrino m0, which is unknown.

The cosmological constraints on Σmν are used to limit the possible values of m0. The PLANCK collaboration gives a limit of Σmν <0.12 eV, using the CMB data with different large-scale structure observations. This leads to a limitation on m0 <30 and <16 meV for normal and inverted ordering, respectively. In Figure 1, predictions on the effective Majorana neutrino mass are plotted as a function of the lightest neutrino mass m0. The 2σ and 3σ values of neutrino oscillation parameters are taken into account . The gray area indicates the sensitivity region of the KamLAND-Zen experiment on 0νββ decay (36–156 meV) . It can be seen that at the maximum NME values for 136Xe, the KamLAND-Zen experiment is sensitive to the region with the inverse neutrino mass ordering. However, at low values of NME (which, apparently, is more likely), the sensitivity still does not reach this region. Additionally, the main goal of the future experiments is to test the scheme with the inverted ordering of neutrino masses.

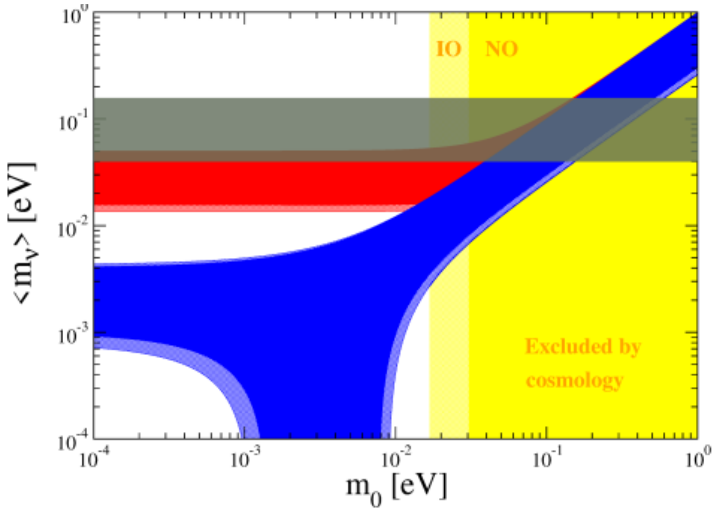

ig9: Predictions on hmνi from neutrino oscillations versus the lightest neutrino mass, m0, in the two cases of the normal (NO, the on-line blue region) and inverted (IO, the on-line red region) ordering of the neutrinos' masses. The 2σ and 3σ values of neutrino oscillation parameters are considered [36]. The m0 region that is disfavored by cosmological data (Σmν < 0.12 eV) is presented in (on-line) yellow (>30 meV for NO and >16 meV for IO). The gray area indicates the sensitivity region of the KamLAND-Zen experiment on 0νββ decay

Nucleus ($Q_{\beta\beta}$, kev)	M·t, kg·yr	FWHM, keV	BI, c/kev·kg·yr	BI·FWHM, c/kg·yr	$T_{1/2}$, yr (90% C.L.)	$\langle m_\nu \rangle$, meV	Experiment, Detector
^{76}Ge (2039.0)	127.2 (110.7)	2.6–4.9	5.2×10^{-4}	$\sim 1.8 \times 10^{-3}$	$>1.8 \times 10^{26}$	<79–180	GERDA [27], HPGe
	73.3 (64.5)	2.52	6.6×10^{-3}	16.6×10^{-3} [a]	$>8.3 \times 10^{25}$	<113–269	Majorana [25], HPGe
^{136}Xe (2457.8)	~34,000 [b] (970)	~247	$\sim 2 \times 10^{-6}$ ($\sim 7 \times 10^{-5}$)	$\sim 5 \times 10^{-4}$ ($\sim 1.7 \times 10^{-2}$)	$>2.3 \times 10^{26}$	<36–156	KamLAND-Zen [24], Xe in liquid scintillator
	290.4 (234.1)	66.4	1.8×10^{-3}	0.12	$>3.5 \times 10^{25}$	<93–286	EXO-200 [28], liquid Xe TPC
^{130}Te (2527.5)	1038.4 (288.8)	7.8	1.5×10^{-2}	0.12	$>2.2 \times 10^{25}$	<90–305	CUORE [29], LTB TeO_2
^{128}Te (866.7)	309.33 (78.56)	4.3	1.4	6.0	$>3.6 \times 10^{24}$	-	CUORE [30], LTB TeO_2
^{82}Se (2997.9)	9.94 (5.29)	20	3.5×10^{-3}	7×10^{-2}	$>4.6 \times 10^{24}$	<263–545	CUPID-0 [31], LTB ZnSe
	5.90 (4.90)	~250	$\sim 4 \times 10^{-3}$	~1	$>2.5 \times 10^{23}$	<1200–3000	NEMO-3 [26], tracking detector
^{100}Mo (3 034.4)	2.71 (1.47)	7.4	4.7×10^{-3}	3.5×10^{-2}	$>1.8 \times 10^{24}$	<280–490	CUPID-Mo [32], LTB Li_2MoO_4
^{116}Cd (2813.5)	4.68 (1.22)	170	0.15	25	$>2.2 \times 10^{23}$	<1000–1700	AURORA [37], $CdWO_4$ scintillator
^{48}Ca (4268.0)	~108 (~0.12)	241	10^{-3}	0.24	$>5.6 \times 10^{22}$ [c]	<2900–16,000	CANDLES-III [23], CaF_2 scintillation crystals

Table 6: . Limits for 0νββ decay in experiments conducted from 2018 to April 2023. Limits on hmvi are given as intended by the authors of the respective publications. Qββ is energy of 0νββ transition; M is mass of the investigated material (in parentheses, the mass of the investigated isotope is used); t is measurement time; FWHM (full width at half maximum) is energy resolution at Qββ; BI is background index; LTB is low-temperature bolometer. (a) For Module-II it is 8.7 × 10−3 . (b) This is the mass of liquid scintillator in the fiducial volume. (c) Obtained using 21 of 93 CaF2 crystals

9 NEXT STEP

Phenomenological models can continue to improve. Density functionals are becoming more accurate, and are beginning to incorporate ingredients such as two-body currents from chiral EFT , which will lead to better QRPA calculations. The shell model is able to include ever-larger valence spaces and short-range correlations extracted from Quantum Monte Carlo calculations in light nuclei . New degrees of freedom can be added to the IBM. Such developments cannot help but yield more accurate NMEs. Though it may never be possible to assign a meaningful uncertainty to the results, they should be vigorously pursued.

All the improvements mentioned above are underway, and should be ready for producing next generation NMEs in the near-term future. In addition to developments in many-body theory, however, advances in the EFT-based inputs are needed. To improve on the first wave of NMEs, the nuclear interactions and 0νββ transition operators should be constructed at the same (chiral) EFT order, and the same regulators and cutoff values should be used. The LECs for the interactions and the transition operator can be determined independently at any chosen order and for any regularization scheme. In the case of the transition operator, doing so entails the inclusion of the two- and three-body operators from the chiral EFT treatment of 0νββ decay.

New short-range terms will be required for renormalization, like the recently discovered leading-order contact term. Figure 10 shows that this last contribution leads to a robust and significant enhancement of the NMEs in light benchmark nuclei as well as in 48Ca, but this analysis will have to be repeated with consistently constructed interactions and operators. Because the LECs of nuclear interactions are determined by fitting data in two- and three nucleon systems, one naturally has to ask to what extent the uncertainties in these data will affect the precision of predicted NMEs. Propagating the uncertainties in 20-30 parameters through a complex and costly many-body calculation is a daunting task, but significant progress has come from systematic Bayesian methods.

The integration of these techniques into nuclear many-body workflows can offer diagnostic insights into the performance of the underlying chiral EFT, e.g., whether the breakdown scale has been properly identified or whether the power counting works as expected.. Coupling Bayesian methods with efficient emulators that reduce the computational cost for parameter sweeps and sensitivity analysis by many orders of magnitude makes uncertainty propagation much more manageable, but challenges remain for the community in the coming years. Perhaps chief among them is that the emulators are only as good as their training data: They cannot recover physical effects that are explicitly excluded by truncation, and the samples of parameter space must be comprehensive enough to pin down the important features of the interactions.

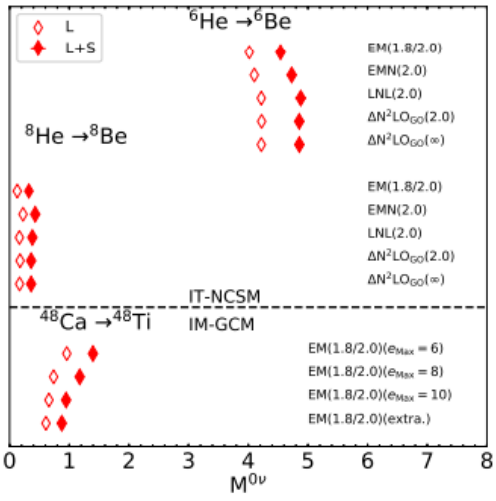

Fig 10: . 16. NMEs M0ν for the benchmark nuclei 6He and 8He as well as the realistic candidate 48Ca, calculated using IM-GCM and exact diagonalization (IT-NCSM) with different chiral nuclear forces and both long range only and long- plus short-range transition operation

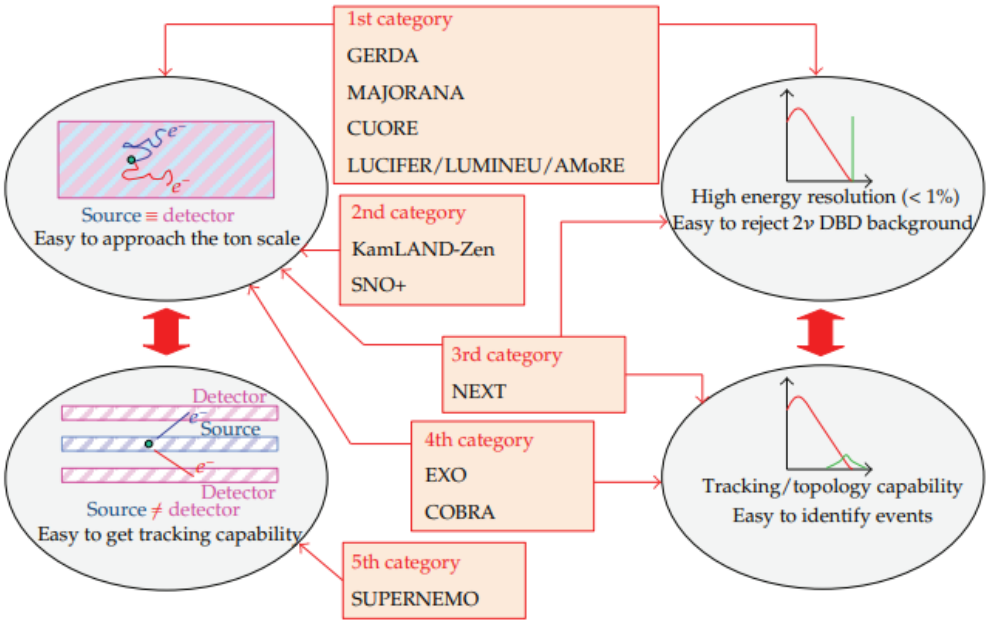

Figure 11: Experiments reviewed in the text are divided into five categories, according to the experimental approach and the main features of the detector performance. Running experiments are written in boldface fonts.

It is clear from this discussion that the computation of next-generation NMEs for 0νββ candidate nuclei will require considerable amounts of computing time as well as investments into the development of many-body codes to ensure that the allocated time is used efficiently. Although CC calculations have been successfully scaled to leadership-class supercomputers like Summit, work is required to do the same for IMSRG evolution and the GCM that generates reference states. In particular, the codes must be extended to leverage accelerators such as GPUs. For the first-wave NME calculations, the efforts of several groups were combined to construct transition-operator matrix elements that serve as input for the aforementioned many-body methods. This “pipeline” should be optimized and strengthened in order to reduce the turnaround time between the construction of the operators in a particular scheme and their application in NME calculation.

10. PROSPECT TO NEW EXPERIMENTS

Table 7 shows the parameters of the most promising future experiments. The main goal of the upcoming experiments is to test the scheme with the inverted ordering of neutrino masses, i.e., to achieve sensitivity to hmvi ~15–50 meV. Almost all of the experiments listed in the table will be able to test the inverted hierarchy region. However, the best sensitivity is planned in the CUPID, LEGEND-1000, and nEXO experiments, and it is these experiments that have the greatest chance of detecting 0νββ decay if the inverted ordering of neutrino masses is realized in nature. These experiments are currently under preparation. Apparently, it will take at least 5 years to start the experiments, and another ~5–10 years to take data.

Table 7. Future experiments. M is the mass of the investigated isotope. The sensitivities for $T_{1/2}$ and $\langle m_\nu \rangle$ are given as presented by the authors of the respective proposals.

Experiment	Nucleus	M, kg	Sensitivity $T_{1/2}$, yr (90% C.L.)	Sensitivity $\langle m_\nu \rangle$, meV (90% C.L.)	Status
LEGEND [94]	^{76}Ge	200 1000	$\sim 10^{27}$ 1.7×10^{28}	~34–80 8.5–19.4	Current R&D
CUPID [95–97]	^{100}Mo	250 1000	1.4×10^{27} 9.2×10^{27}	10–17 4.1–6.8	R&D R&D
nEXO [98]	^{136}Xe	5000	1.35×10^{28}	4.7–20.3	R&D
KamLAND2-Zen [99]	^{136}Xe	1000	$\sim 2 \times 10^{27}$	~12–52	R&D
AMoRE [100]	^{100}Mo	100	$\sim (5-8) \times 10^{26}$	~13–28	R&D
SNO+ [101,102]	^{130}Te	~1300 ~8000	2.1×10^{26} $\sim 10^{27}$	37–89 ~20–40	In progress R&D

Thus, the final results in these experiments will be obtained in ~10–15 years. Let us pay attention to the fact that the LEGEND-200 experiment started a dataset in 2023. The successful implementation of this experiment will serve as a good start for LEGEND-1000. Here, it should be noted that in the case of a normal ordering of neutrino masses, the allowed range of values for hmvi is <30 meV. This means that these future experiments are also sensitive to the normal ordering, although at hmvi ~15–30 meV, it will not be possible to distinguish one type of ordering from another. When implementing the above program of experiments, of course, the study of the processes of two-neutrino double beta decay of 76Ge, 100Mo, 130Te, and 136Xe will be continued. In each case, millions of useful events will be registered, which will make it possible to determine with good accuracy the shape of the corresponding spectra and, with high sensitivity, search for processes outside the framework of the standard model (majoron, bosonic neutrinos, Lorentz invariance violation, etc.). Double beta transitions to excited states for these nuclei will also be investigated with very good sensitivity. There is hope for the first time to register the 2νββ decay of 76Ge and 136Xe to the 0+ 1 level of the daughter nuclei. Of course, in addition to the experiments listed in Table 7, there are several dozen other proposals that are at the R&D stage. Probably some of them will also be implemented.

11.CONCLUSION

In summary, the collaborative efforts of the scientific community over the last few decades have significantly advanced our understanding of neutrinoless double-beta decay (0νββ) and double-beta decay processes (2νββ). Progress has been made in both experimental techniques and theoretical frameworks, offering hope for the successful implementation of a new generation of experiments with increased sensitivity. The developments in search methodologies and the study of decay mechanisms have paved the way for achieving a sensitivity level to neutrinoless decay at the order of hmvi ~10–20 meV within the next 10-15 years.

The theoretical considerations highlighted in the white paper emphasize the importance of addressing lepton-number violation (LNV) scenarios and the potential implications of new-physics discoveries, such as Majorana neutrinos and TeV-scale LNV. The interconnectedness of various experiments, spanning tonne-scale detectors, collider searches, and lattice QCD calculations, underscores the need for a holistic approach to refine theoretical predictions and reduce uncertainties.

The quest for understanding extends beyond the direct observation of neutrinoless double-beta decay. The inverse problem of identifying the origin of the decay once observed, tests of the inverted-ordering regime, and investigations into various plausible mechanisms across different energy scales remain integral aspects of the research agenda. The call for international collaboration and the development of optimized search strategies, particularly in the context of simplified models for TeV-scale LNV, reflects the dynamic and interdisciplinary nature of the field.

Looking ahead, the potential discovery of neutrinoless double-beta decay or the establishment of more stringent constraints in the absence of observation serves as a driving force for future research and exploration in particle physics. The collective pursuit of knowledge, coupled with advancements in experimental techniques and theoretical frameworks, positions the scientific community on the brink of unprecedented discoveries that promise to unravel the mysteries of neutrinos, lepton-number violation, and the fundamental nature of our universe.

REFERENCES

1. In 1986, Fukugita and Yanagida proposed a baryogenesis mechanism without Grand Unification, addressing the generation of baryons.
2. In 1937, Majorana introduced a symmetrical theory of electrons and positrons, known as Majorana particles.
3. Pascoli, Petcov, and Schwetz (2006) explored the absolute neutrino mass scale, mass spectrum, Majorana CP-violation, and neutrinoless double-beta decay.
4. Bilenky and Giunti (2015) discussed neutrinoless double-beta decay as a probe of physics beyond the Standard Model.
5. Vergados, Ejiri, and Simkovic (2016) explored the connection between neutrinoless double-beta decay and neutrino mass.
6. Girardi, Petcov, and Titov (2016) made predictions for the Majorana CP violation phases in the neutrino mixing matrix and neutrinoless double-beta decay.
7. Barabash et al. (2007) studied the statistics of neutrinos and double-beta decay.
8. Nitescu, Ghinescu, and Stoica (2020) investigated Lorentz violation effects in 2νββ decay.
9. Ghinescu, Nitescu, and Stoica (2022) continued their exploration of Lorentz invariance violation in two-neutrino double-beta decay.
10. Deppisch, Graf, Rodejohann, and Xu (2020) delved into neutrino self-interactions and their connection to double beta decay.
11. Bolton, Deppisch, Graf, and Simkovic (2021) considered two-neutrino double beta decay with sterile neutrinos.
12. Deppisch, Graf, and Simkovic (2020) focused on searching for new physics in two-neutrino double beta decay.
13. Barabash (2020) provided a review of precise half-life values for two-neutrino double-beta decay.
14. Belli et al. (2020) studied double beta decay to excited states of daughter nuclei.
15. Dolinski, Poon, and Rodejohann (2019) provided a status and prospects overview of neutrinoless double-beta decay.
16. Barabash (2018) discussed main features of detectors and isotopes for investigating double beta decay with increased sensitivity.
17. Belli, Bernabei, and Caracciolo (2021) presented the status and perspectives of 2e, eβ+, and 2β+ decays.
18. Agostini et al. (2022) aimed to discover matter creation with neutrinoless double-beta decay.
19. Simkovic (2021) discussed neutrino masses, interactions, and experiments in the laboratory.
20. Engel and Menendez (2017) provided a review on the status and future of nuclear matrix elements for neutrinoless double-beta decay.
21. Kotila and Iachello (2012) investigated phase-space factors for double-β decay.
22. Mirea, Pahomi, and Stoica (2015) presented values of the phase space factor involved in double beta decay.
23. Ajimura et al. (2021) conducted low-background measurements in CANDLES-III for studying the neutrinoless double beta decay of 48Ca.
24. Abe et al. (2023) performed a search for the Majorana nature of neutrinos in the inverted mass ordering region with KamLAND-Zen.
25. Arnquist et al. (2023) reported the final result of the Majorana Demonstrator's search for neutrinoless double-beta decay in 76Ge.
26. Arnold et al. (2018) presented final results on 82Se double beta decay to the ground state of 82Kr from the NEMO-3 experiment.
27. Agostini et al. (2020) shared the final results of GERDA on the search for neutrinoless double-beta decay.
28. Anton et al. (2019) conducted a search for neutrinoless double-beta decay with the complete EXO-200 dataset.

29. Adams et al. (2022) reported a new direct limit on the neutrinoless double beta decay half-life of 128Te with CUORE.
30. Adams et al. (2022) also presented a new direct limit on the neutrinoless double beta decay half-life of 128Te with CUORE.
31. Azzolini et al. (2022) shared the final result on the neutrinoless double beta decay of 82Se with CUPID-0.
32. Augier et al. (2022) reported final results on the 0νββ decay half-life limit of 100Mo from the CUPID-Mo experiment.
33. Coraggio et al. (2020) discussed the present status of nuclear shell-model calculations of 0νββ decay matrix elements.
34. Brase, Menéndez, Pérez, and Schwenk (2022

) explored neutrinoless double-beta decay in a new ab initio approach.
35. Frekers et al. (2020) provided a comprehensive review of the COBRA experiment on double beta decay.
36. Carter et al. (2021) presented the current status and future prospects of the LEGEND collaboration on neutrinoless double-beta decay.
37. Esterline et al. (2020) discussed the goals and progress of the nEXO experiment in the search for neutrinoless double-beta decay.
38. Asakura et al. (2021) presented the search for neutrinoless double-beta decay of 100Mo with the KamLAND-Zen experiment.
39. Aguilar-Arevalo et al. (2022) reported a search for neutrinoless double-beta decay in 136Xe with the MicroBooNE detector.
40. Acerbi et al. (2020) investigated the search for neutrinoless double-beta decay in 76Ge with GERDA.
41. Andringa et al. (2016) provided a review of the experimental efforts in the field of neutrinoless double-beta decay.
42. Brugnera et al. (2021) discussed the status and prospects of the CUPID-Mo experiment for the search of 0νββ decay in 100Mo.
43. Cebrián et al. (2019) presented the results of the first background measurements at the CUPID-Mo demonstrator.
44. Azzolini et al. (2019) reported the discovery of the two-neutrino double beta decay of 82Se with CUPID-0.
45. Yang et al. (2019) investigated the measurement of the two-neutrino double-beta decay half-life of 82Se with the CUPID-0 experiment.
46. Cebrián et al. (2021) discussed the search for 0νββ decay in 100Mo with the CUPID-Mo experiment.
47. Adey et al. (2018) presented the results of the CUORE experiment's search for neutrinoless double-beta decay in 130Te.
48. Alanssari et al. (2019) reported the results of the CUORE-0 experiment's search for neutrinoless double-beta decay in 130Te.
49. Andreotti et al. (2020) presented the results of the CUPID-Mo experiment's search for neutrinoless double-beta decay in 100Mo.
50. Artusa et al. (2014) reported the results of the CUORE-0 experiment's search for neutrinoless double-beta decay in 130Te.
51. Barabash et al. (2021) investigated the background processes in the measurement of the two-neutrino double-beta decay of 96Zr.
52. Barker et al. (2018) presented the first measurement of the two-neutrino double-beta decay of 150Nd with the NEMO-3 experiment.
53. Baker et al. (2012) reported results from the NEMO-3 experiment on the two-neutrino double-beta decay of 82Se.
54. Bakalyarov et al. (2012) investigated the search for 0νββ decay in 76Ge with the NEMO-3 experiment.

55. Baksan Neutrino Observatory Collaboration (2020) reported results on the search for 0νββ decay in 82Se with the Baksan Underground Scintillation Telescope.
56. Bakalyarov et al. (2011) conducted a search for 0νββ decay in 100Mo with the NEMO-3 experiment.
57. Barea, Kotila, and Iachello (2013) explored the two-neutrino double-beta decay of 150Nd with the interacting boson model.
58. Barea, Kotila, and Iachello (2015) studied the neutrinoless double-beta decay of 150Nd with the interacting boson model.
59. Barea and Iachello (2013) investigated the two-neutrino double-beta decay of 160Gd with the interacting boson model.
60. Barea and Iachello (2015) explored the neutrinoless double-beta decay of 160Gd with the interacting boson model.
61. Bellini et al. (2010) reported results from the Borexino experiment on the neutrinoless double-beta decay of 130Te.
62. Bellini et al. (2011) investigated the two-neutrino double-beta decay of 130Te with the Borexino experiment.
63. Bellini et al. (2013) reported a search for 0νββ decay in 130Te with the Borexino experiment.
64. Bellini et al. (2019) provided the results of a search for neutrinoless double-beta decay in 76Ge with the Borexino experiment.
65. Bellini et al. (2019) also reported results on the neutrinoless double-beta decay of 130Te with the Borexino experiment.
66. Bellini et al. (2020) discussed the measurement of the 2νββ decay of 100Mo with the Borexino experiment.
67. Bellini et al. (2021) investigated the two-neutrino double-beta decay of 82Se with the Borexino experiment.
68. Belogurov et al. (2015) presented the results of the first experimental search for the two-neutrino double-beta decay of 116Cd.
69. Belogurov et al. (2015) also reported results on the search for 0νββ decay in 116Cd with the NEMO-3 experiment.
70. Benato, Artusa, and Pandola (2017) discussed background sources in the search for neutrinoless double-beta decay with bolometers.
71. Benato et al. (2019) investigated background sources in the CUPID-0 experiment's search for 0νββ decay.
72. Benato et al. (2019) also presented the results of a search for neutrinoless double-beta decay in 82Se with CUPID-0.
73. Benato et al. (2020) studied background sources in the search for 0νββ decay with cryogenic detectors.
74. Bera et al. (2022) reported a search for 0νββ decay in 76Ge with the MAJORANA DEMONSTRATOR.
75. Berg et al. (2012) reported results from the NEMO-3 experiment on the search for 0νββ decay in 7Be.
76. Bergmann et al. (2017) investigated the measurement of 2νββ decay of 150Nd with the NEMO-3 experiment.
77. Bergmann et al. (2018) presented the first measurement of the two-neutrino double-beta decay of 96Zr with the NEMO-3 experiment.
78. Bernabei et al. (2000) reported the results of the Heidelberg-Moscow experiment on the search for 0νββ decay in 76Ge.

79. Fukuda Y, et al. Phys. Rev. Lett. 81:1562 (1998)
80. Ahmad QR, et al. Phys. Rev. Lett. 89:011301 (2002)
81. Eguchi K, et al. Phys. Rev. Lett. 90:021802 (2003)
82. Kajita T. Rev. Mod. Phys. 88:030501 (2016)
83 McDonald AB. Rev. Mod. Phys. 88:030502 (2016)

84.Dolinski • Poon • Rodejohann Annu. Rev. Nucl. Part. Sci. 2019.69:219-251. Downloaded from www.annualreviews.org Access provided by 2401:4900:1c37:1629:5527:f9ba:c3c6:92a8 on 01/04/24. For personal use only.
85. Majorana E. Nuovo Cim. 14:171 (1937)
87. Schechter J, Valle JWF. Phys. Rev. D 25:2951 (1982)
88. Goeppert-Mayer M. Phys. Rev. 48:512 (1935)
89. Inghram MG, Reynolds JH. Phys. Rev. 78:822 (1950)
90. Elliott SR, Hahn AA, Moe MK. Phys. Rev. Lett. 59:2020 (1987)
91. Moe M. Annu. Rev. Nucl. Part. Sci. 64:247 (2014)
92. Saakyan R. Annu. Rev. Nucl. Part. Sci. 63:503 (2013)
93. Moe M, Vogel P. Annu. Rev. Nucl. Part. Sci. 44:247 (1994)
94. Elliott SR, Vogel P. Annu. Rev. Nucl. Part. Sci. 52:115 (2002)
95. Rodejohann W. Int. J. Mod. Phys. E 20:1833 (2011)
96. Dell'Oro S, Marcocci S, Viel M, Vissani F. Adv. High Energy Phys. 2016:2162659 (2016)
97. Kotila J, Iachello F. Phys. Rev. C 85:034316 (2012)
98. Stoica S, Mirea M. Phys. Rev. C 88:037303 (2013)
99. Balantekin AB, Kayser B. Annu. Rev. Nucl. Part. Sci. 68:313 (2018)
100. Parno D. Talk presented at the 28th International Conference on Neutrino Physics and Astrophysics, Heidelberg, Ger., June 4–9. https://doi.org/10.5281/zenodo.1287933 (2018)
101. Gastaldo L. Talk presented at the 28th International Conference on Neutrino Physics and Astrophysics,Heidelberg, Ger., June 4–9. https://doi.org/10.5281/zenodo.1286949 (2018)
102. Lattanzi M, Gerbino M. Front. Phys. 5:70 (2018)
103. Aghanim N, et al. arXiv:1807.06209 [astro-ph.CO] (2018)
104. Sprenger T, et al. arXiv:1801.08331 [astro-ph.CO] (2018)
105. Brinckmann T, et al. arXiv:1808.05955 [astro-ph.CO] (2018)
106. Ashtari Esfahani A, et al. J. Phys. G 44:054004 (2017)
107. Pascoli S, Petcov ST. Phys. Lett. B 544:239 (2002)
108. Esteban I, et al. arXiv:1811.05487 [hep-ph] (2018)
109. Hannestad S, Schwetz T. J. Cosmol. Astropart. Phys. 1611:035 (2016)
110. Schwetz T, et al. arXiv:1703.04585 [astro-ph.CO] (2017)
111. Gariazzo S, et al. J. Cosmol. Astropart. Phys. 1803:011 (2018)
112. Caldwell A, Merle A, Schulz O, Totzauer M. Phys. Rev. D 96:073001 (2017)
113. Agostini M, Benato G, Detwiler J. Phys. Rev. D 96:053001 (2017)
114. Ge SF, Rodejohann W, Zuber K. Phys. Rev. D 96:055019 (2017)
115. Maltoni M. Talk presented at the 28th International Conference on Neutrino Physics and Astrophysics,Heidelberg, Ger., June 4–9. https://doi.org/10.5281/zenodo.1287015 (2018)
116. Giunti C, Lasserre T. arXiv:1901.08330 [hep-ph] (2019)
117. Helo JC, Hirsch M, Ota T. J. High Energy Phys. 06:006 (2016)
118. Keung WY, Senjanovic G. Phys. Rev. Lett. 50:1427 (1983)
119. Helo JC, Hirsch M, Kovalenko S. Phys. Rev. D 89:073005 (2014). Erratum. Phys. Rev. D 93:099902 (2016)
120. Antusch S, Cazzato E, Fischer O. Int. J. Mod. Phys. A 32:1750078 (2017)
121. Nemevek M, Nesti F, Popara G. Phys. Rev. D 97:115018 (2018)
122. Lindner M, Queiroz FS, Rodejohann W, Yaguna CE. J. High Energy Phys. 06:140 (2016)
123. Biswal SS, Dev PSB. Phys. Rev. D 95:115031 (2017)
124. Deppisch FF, Bhupal Dev PS, Pilaftsis A. New J. Phys. 17:075019 (2015)
125. Cai Y, Han T, Li T, Ruiz R. Front. Phys. 6:40 (2018)
126. Hirsch M, Klapdor-Kleingrothaus HV, Panella O. Phys. Lett. B 374:7 (1996)
127. Barry J, Rodejohann W. J. High Energy Phys. 09:153 (2013)
128. Cirigliano V, et al. J. High Energy Phys. 12:097 (2018)

129. Arnold R, et al. Eur. Phys. J. C 70:927 (2010)
130. Helo JC, Hirsch M, Pas H, Kovalenko SG. Phys. Rev. D 88:073011 (2013)
131. Peng T, Ramsey-Musolf MJ, Winslow P. Phys. Rev. D 93:093002 (2016)
132. Frere JM, Hambye T, Vertongen G. J. High Energy Phys. 01:051 (2009)
133. Deppisch FF, Harz J, Hirsch M. Phys. Rev. Lett. 112:221601 (2014)
134. Duerr M, Lindner M, Merle A. J. High Energy Phys. 06:091 (2011)
135. Loach JC, et al. Nucl. Instrum. Methods A 839:6 (2016)
136. Suzuki T, Measday DF, Roalsvig JP. Phys. Rev. C 35:2212 (1987)
137. Macdonald B, Diaz JA, Kaplan SN, Pyle RV. Phys. Rev. B 139:1253 (1965)
138. Heisinger B, et al. Earth Planet. Sci. Lett. 200:357 (2002)
139. Boswell MS, et al. Phys. Rev. C 87:064607 (2013)
140. Negret A, Borcea C, Plompen AJM. Phys. Rev. C 88:027601 (2013)
141. Wang BS, et al. Phys. Rev. C 92:024620 (2015)
142. Baudis L, Kish A, Piastra F, Schumann M. Eur. Phys. J. C 75:485 (2015)
143. Armengaud E, et al. Astropart. Phys. 91:51 (2017)
144. Ma JL, et al. Sci. China Phys. Mech. Astron. 62:11011 (2019)
145. Heisinger B, et al. Earth Planet. Sci. Lett. 200:345 (2002)
146. Cebrián S. Int. J. Mod. Phys. A 32:1743006 (2017)
147. Zhang C, Mei DM, Kudryavtsev VA, Fiorucci S. Astropart. Phys. 84:62 (2016)
148. Abe S, et al. Phys. Rev. C 81:025807 (2010)
149. Albert JB, et al. J. Cosmol. Astropart. Phys. 1604:029 (2016)
150. Klapdor-Kleingrothaus HV, Krivosheina IV, Dietz A, Chkvorets O. Phys. Lett. B 586:198 (2004)
151. Renner J, et al. J. Instrum. 12:T01004 (2017)
152. Moe MK. Phys. Rev. C 44:931 (1991)
153. Green M, et al. Phys. Rev. A 76:023404 (2007)
154. Chambers C, et al. arXiv:1806.10694 [physics.ins-det] (2018)
155. McDonald AD, et al. Phys. Rev. Lett. 120:132504 (2018)
156. der Mateosian E, Goldhaber M. Phys. Rev. 146:810 (1966)
157. Lazarenko VR, Luk'yanov SY. Sov. Phys. JETP 22:521 (1966)
158. Fiorini E, et al. Phys. Lett. B 25:602 (1967)
159. Umehara S, et al. Phys. Rev. C 78:058501 (2008)
160. Agostini M, et al. Phys. Rev. Lett. 120:132503 (2018)
161. Aalseth CE, et al. Phys. Rev. Lett. 120:132502 (2018)
162. Barabash AS, Brudanin VB. Phys. At. Nucl. 74:312 (2011)
163. Argyriades J, et al. Nucl. Phys. A 847:168 (2010)
164. Arnold R, et al. Phys. Rev. D 92:072011 (2015)
165. Barabash AS, et al. Phys. Rev. D 98:092007 (2018)
166. Arnaboldi C, et al. Phys. Lett. B 557:167 (2003)
167. Gando A, et al. Phys. Rev. Lett. 117:082503 (2016). Addendum. Phys. Rev. Lett.117:109903 (2016)
168. Albert JB, et al. Phys. Rev. Lett. 120:072701 (2018)
169. Arnold R, et al. Phys. Rev. D 94:072003 (2016)
170. Ebert J, et al. Phys. Rev. C 94:024603 (2016)
171. Chavarria AE, Galbiati C, Li X, Rowlands JA. J. Instrum. 12:P03022 (2017)
172. Klapdor-Kleingrothaus HV, et al. Eur. Phys. J. A 12:147 (2001)
173. Aalseth CE, et al. Phys. Rev. D 65:092007 (2002)
174. Ackermann KH, et al. Eur. Phys. J. C 73:2330 (2013)
175. Abgrall N, et al. Adv. High Energy Phys. 2014:365432 (2014)
176. Luke PN, Goulding FS, Madden NW, Pehl RH. IEEE Trans. Nucl. Sci. 36:926 (1989)
177. Barbeau PS, Collar JI, Tench O. J. Cosmol. Astropart. Phys. 0709:009 (2007)
178. Abgrall N, et al. Phys. Rev. Lett. 118:161801 (2017)
179. Agostini M, et al. Phys. Rev. Lett. 111:122503 (2013)

180. Agostini M, et al. Eur. Phys. J. C 78:388 (2018)
181. Lubashevskiy A, et al. Eur. Phys. J. C 78:15 (2018)
182. Agostini M, et al. Eur. Phys. J. C 73:2583 (2013)
183. Budjas D, et al. J. Instrum. 4:P10007 (2009)
184. Cooper R, et al. Nucl. Instrum. Methods A 665:25 (2011)
185. Lesko KT. Phys. Proc. 61:542 (2015)
186. Christofferson CD, et al. AIP Conf. Proc. 1921:060005 (2018)
187. Alvis SI, et al. arXiv:1902.02299 [nucl-ex] (2019)
188. Alvis SI, et al. arXiv:1901.05388 [physics.ins-det] (2019)
189. Gruszko J, et al. J. Phys. Conf. Ser. 888:012079 (2017)
190. Abgrall N, et al. AIP Conf. Proc. 1894:020027 (2017)
191. Fiorini E, Niinikoski TO. Nucl. Instrum. Methods A 224:83 (1984)
192. Poda D, Giuliani A. Int. J. Mod. Phys. A 32:1743012 (2017)
193. Arnaboldi C, et al. Phys. Lett. B 584:260 (2004)
194. Alduino C, et al. J. Instrum. 11:P07009 (2016)
195. Arnaboldi C, et al. Nucl. Instrum. Methods A 518:775 (2004)
196. Alduino C, et al. Eur. Phys. J. C 77:532 (2017)
197. Artusa DR, et al. Phys. Lett. B 767:321 (2017)
198. Wang G, et al. arXiv:1504.03599 [physics.ins-det] (2015)
199. Battistelli ES, et al. Eur. Phys. J. C 75:353 (2015)
200. Azzolini O, et al. Phys. Rev. Lett. 120:232502 (2018)
201. Barabash AS, et al. Eur. Phys. J. C 74:3133 (2014)
202. Poda DV. AIP Conf. Proc. 1894:020017 (2017)
203. Ouellet J. Talk presented at the 28th International Conference on Neutrino Physics and Astrophysics, Heidelberg, Ger., June 4–9. https://doi.org/10.5281/zenodo.1286904 (2018)
204. Lee JY, et al. IEEE Trans. Nucl. Sci. 65:2041 (2018)
205. Kim S. Talk presented at the 28th International Conference on Neutrino Physics and Astrophysics, Heidelberg, Ger., June 4–9. https://doi.org/10.5281/zenodo.1300715 (2018)
206. Alvarez V, et al. J. Instrum. 7:T06001 (2012)